AI-Compass: A Comprehensive and Effective Multi-module Testing Tool for AI Systems

Zhiyu Zhu*, Zhibo Jin*, Hongsheng Hu, Minhui Xue, Ruoxi Sun, Seyit Camtepe, Praveen Gauravaram, and Huaming Chen†

Abstract—AI systems, in particular with deep learning techniques, have demonstrated superior performance for various real-world applications. Given the need for tailored optimization in specific scenarios, as well as the concerns related to the exploits of subsurface vulnerabilities, a more comprehensive and in-depth testing AI system becomes a pivotal topic. We have seen the emergence of testing tools in real-world applications that aim to expand testing capabilities. However, they often concentrate on ad-hoc tasks, rendering them unsuitable for simultaneously testing multiple aspects or components. Furthermore, trustworthiness issues arising from adversarial attacks and the challenge of interpreting deep learning models pose new challenges for developing more comprehensive and in-depth AI system testing tools. In this study, we design and implement a testing tool, AI-COMPASS, to comprehensively and effectively evaluate AI systems. The tool extensively assesses multiple measurements towards adversarial robustness, model interpretability, and performs neuron analysis. The feasibility of the proposed testing tool is thoroughly validated across various modalities, including image classification, object detection, and text classification. Extensive experiments demonstrate that AI-COMPASS is the state-of-the-art tool for a comprehensive assessment of the robustness and trustworthiness of AI systems. Our research sheds light on a general solution for AI systems testing landscape.

Index Terms—Deep learning testing tool, adversarial robustness, model interpretability, neuron analysis.

1 INTRODUCTION

In recent years, the remarkable improvement of deep learning models have revolutionized the landscape of various industry sectors and application domains, showcasing their unparalleled potential in solving complex problems and driving innovation [1]–[8]. The dynamic interplay between data-driven insights and sophisticated model architectures has propelled deep learning to the forefront of modern technology, enabling groundbreaking advancements across a myriad of novel applications [9]–[11]. From enhancing medical diagnostics through image analysis to enabling autonomous vehicles to navigate and make informed decisions, the transformative capabilities of deep learning models have left an indelible mark on society [12]–[15]. To contextualize this transformative power, consider the case of natural language processing where models like GPT-3 have demonstrated human-level proficiency in generating coherent and contextually relevant text, ushering in a new era of interactive and responsive AI systems [16], [17]. Such remarkable feats underscore the urgent need for a comprehensive assessment framework that can holistically evaluate the multifaceted dimensions of deep learning models, delving into the intricate interplay of vast datasets, intricate model architectures, and immense computational resources that underpin their unprecedented success [18]–[20].

The comprehensive assessment of deployed machine learning (ML) models, particularly deep learning models, is of paramount importance [21]. Such assessments serve as a crucial precautionary measure to uncover potential pitfalls and unanticipated consequences that could arise from utilizing inadequately evaluated models [22], [23]. Conducting a thorough performance and security evaluation ensures a nuanced understanding of the models' capabilities, limitations, and potential biases, empowering informed decision-making and responsible deployment [24]. Neglecting a comprehensive assessment when deploying deep learning models can lead to detrimental outcomes. Biased predictions, unreliable results, and unexpected behaviors may emerge, eroding user trust, triggering legal and ethical challenges, and compromising the models' real-world performance [25]. Real-world examples vividly illustrate these perils. In healthcare, deploying a poorly assessed AI diagnostic system could endanger patients through misdiagnoses [26]. For instance, malicious actors may mislead the ML tumor detection system into erroneously classifying benign tumors as malignant ones by introducing imperceptible perturbations to the original medical images. This has the potential to misguide the physician's judgment, subsequently leading to irreversible harm to the patient's health [27]. While inadequately evaluated autonomous vehicles might make flawed decisions, resulting in accidents [28]. For example, attackers can launch attacks on autonomous driving systems by introducing imperceptible perturbations to traffic signs. By applying imperceptible perturbations to stop signs as perceived by human eyes, the ML system may misclassify them as yield signs. This

Zhiyu Zhu and Zhibo Jin are with the School of Electrical and Computer Engineering, The University of Sydney and CSIRO's Data61 (e-mail: {zzhu2018, zjin0915}@uni.sydney.edu.au
Huaming Chen is with the School of Electrical and Computer Engineering, The University of Sydney (e-mail: {huaming.chen, tj.lim}@sydney.edu.au).
Hongsheng Hu, Minhui Xue, Ruoxi Sun, and Seyit Camtepe are with CSIRO's Data61 and Cybersecurity CRC (e-mail: {hongsheng.hu, jason.xue, ruoxi.sun, seyit.camtepe}@data61.csiro.au.
Praveen Gauravaram is with Cybersecurity CRC.
**Equal contribution.*
†*Corresponding author.*

could lead to severe traffic accidents, posing a threat to user safety [29]. The financial sector is also at risk, as untested deep learning algorithms in market predictions could yield severe economic repercussions [30]. These instances underscore the urgency of a robust assessment framework, which is essential for mitigating risks and ensuring the safe and effective deployment of deep learning models [31].

To achieve a comprehensive assessment of deep models, it is imperative to delve into three pivotal dimensions: adversarial robustness, model explainability, and neuron analysis [32]–[34]. Adversarial robustness stands as a bulwark, ensuring consistent performance even amid uncertainties and adversarial scenarios, thus fortifying its real-world applicability [35]. Meanwhile, model explainability serves as a beacon of transparency, demystifying the decision-making process and fostering trust, especially in contexts where accountability is paramount [36]. Simultaneously, the intricate realm of neuron analysis grants us a profound understanding of the model's inner workings, at the level of individual neurons, elucidating the pathways of feature extraction and representation learning [37]. The convergence of these facets not only empowers a comprehensive evaluation but also equips stakeholders with the insights needed to navigate the nuanced landscape of deep learning models, promoting informed deployment and harnessing their transformative potential across diverse domains [38].

In order to enhance the capability for testing Deep Learning Systems (DLS) in real-world applications, numeric testing tools have been developed. Taking medical image analysis as an example, DLTK [39], as an open-source DL toolkit, provides a range of tools for testing and validating the quality of DLS, including model evaluation, model interpretation, and model visualization. DLTK provides a detailed diagnostic report for medical images, reducing the risk of misjudgment by explaining the model's behavior. DeepXplore [40] is an automated white-box testing framework for DLS that employs optimization techniques such as gradient ascent to detect potential failures in the system. As an effective approach for automated testing of deep neural network (DNN)-driven autonomous cars, DeepTest [41] designs a test generation framework that combines mutation operators, metamorphic relations, and real-world driving scenarios to generate test cases with higher neuron coverage. However, even though the DLS testing tools are constantly being upgraded, resembling an arms race in multiple fields as described above, the inherent ad-hoc, task-oriented nature of existing tools persists as an unavoidable limitation, often making them unsuitable for fulfilling multi-task testing requirements. For example, the testing objective of DeepXplore is monotonous, and it is exclusively applicable to white-box testing, which makes it unsuitable as a general-purpose testing tool in a black-box environment. Furthermore, DeepXplore does not provide an explanation for how a model's defects are detected. Both DLTK and DeepTest have limited testing capabilities in application scenarios unrelated to medical image analysis and DNN-driven autonomous driving, lacking sufficient tests of adversarial robustness or model interpretability. As far as we know, existing testing tools can only conduct individual module tests on a model's adversarial robustness, interpretability, or neuron analysis, rather than explaining the relationships among these three aspects. In order to enable multidimensional evaluation and selection of models, we are dedicated to integrating these modules for multi-task testing and constructing a comprehensive testing tool. In addition, pruning has been proven to facilitate the interpretation of model decisions and reduce the occurrence of overfitting during adversarial sample training [42], [43]. For the first time, we introduce an approach to neuron analysis with pruning techniques, thereby exploring potential connections among the modules.

In this paper, we propose AI-COMPASS, a comprehensive and effective multi-module testing tool for DLS. Specifically, combined with the basic utility module including indicator evaluation and mutation operations [44], [45], for the first time, we design modules for adversarial robustness, model interpretability and neuron analysis, to extensively evaluate the performance of DLS [46]. Through a thorough validation involving 6 deep learning models across 3 datasets, we demonstrate that AI-COMPASS is capable of testing image classification, object detection, and text classification tasks in DLS. Compared to existing DLS testing tools, AI-COMPASS not only conducts fundamental DLS testing but also delivers precise evaluations of model robustness against adversarial attacks. Furthermore, it provides trustworthy model interpretability reports, including a quantified assessment of the tested model's interpretability, along with attributional result charts for illustration.

The main contributions of this paper are as follows:

- We present a comprehensive and effective framework, AI-COMPASS, for automatically testing the quality of DLS. Specifically, combined with the basic utility module, for the first time, we design modules for adversarial robustness, model interpretability, and neuron analysis, making a significant step towards building robust and trustworthy DLS.
- Inspired by the pruning algorithm, we conduct an in-depth analysis of neural network redundancy. We comprehensively investigate the changes in adversarial robustness and model interpretability resulting from neuron pruning approach, thus providing valuable insights for model architecture optimization.
- We demonstrate that our AI-COMPASS can be effectively applied for multi-modal scenarios. The testing results in image classification, text classification, and object detection tasks verify the high scalability of our AI-COMPASS and solve the ad-hoc problem in existing testing tools.
- We have conducted extensive experiments and generated detailed test reports to demonstrate the superiority of our AI-COMPASS in testing DLS.
- The code is released for future research and enhancements by scholars and industry professionals.

This study extends our previous conference paper [46]. In Section 2, we provide an overview of related work on testing frameworks to afford readers a more comprehensive understanding of the field. Section 3 introduces the preparatory background, furnishing foundational knowledge regarding adversarial attacks, model interpretability, and pruning algorithms. In Section 4, we expand the conceptual diagram of ML-compass [46] to assist readers in

TABLE 1
Existing testing tools for DLS assessment

	Basic Metric	Mutants	Neural Analysis	Robustness Analysis (white-box)	Robustness Analysis (black-box)	Interpretability	Multi-Model
DeepXplore [40]	●	○	●	●	○	○	○
NeuronFair [47]	●	○	○	○	○	●	○
DeepGauge [48]	●	○	○	○	○	○	○
DeepTest [41]	●	○	○	○	○	○	○
DeepMutation [44]	●	●	○	○	○	○	○
DeepMutation++ [45]	●	●	○	●	○	○	○
InterpretDL [49]	○	○	○	○	○	●	○
Ours (AI-Compass)	●	●	●	●	●	●	●

●: The test tool has the function; ○: The test tool does not have the function.

gaining a clearer and more comprehensive grasp of the AI-COMPASS architecture. Section 5 delves into the methods and principles underpinning each module and submodule to provide a more profound understanding of the framework's foundational principles. Section 6 explains the experimental setup and analyzes the experimental results.

In this study, we primarily undertake the following innovations in expending ML-compass:

- Involving more metrics in model utility evaluation.
- Introducing mutant methods in the model utility evaluation to simulate real-world scenarios.
- Incorporating black-box transfer attacks in the robustness evaluation to reveal potential model vulnerabilities in practice.
- Integrating more interpretability methods in the interpretability evaluation, using Insertion & Deletion Score as a metric to quantitatively assess model interpretability.
- To enable neuron analysis, we employed additional pruning algorithms.
- Introducing a comprehensive evaluation, utilizing radar charts for a more intuitive display of model testing results, facilitating user selection of suitable models.
- Exploring additional testing possibilities for models by combining pruning algorithms with the robustness and interpretability analysis.

2 RELATED WORK

In this section, we introduce the existing testing tools for assessing deep learning models. Based on their functionalities, existing DLS testing tools could be categorized into three groups, focusing on adversarial robustness, model interpretability, and neuron analysis, separately.

Testing tools for adversarial robustness. Adversarial attacks refer to malicious attempts by adversaries to introduce subtle yet meaningful perturbations to input data, with the aim of inducing misclassification or erroneous predictions from the model. Currently, mainstream adversarial attacks can be categorized into white-box attacks and black-box attacks. In a white-box setting, relevant information such as the structure and parameters of the target model are transparent. Leveraging this characteristic, white-box attack algorithms can generate high-quality adversarial examples to assess the target model's resilience against various types of attacks. Therefore, white-box attacks serve as an ideal approach to evaluate the robustness of models against adversarial attacks. By continuously challenging and attacking models, researchers and software developers can uncover and address hidden flaws, thereby contributing to the construction of more secure and reliable DLS that safeguard the security of users and data. The Adversarial Robustness Toolbox (ART) [50] is an open-source testing tool dedicated to evaluating and enhancing the robustness of deep learning models. It offers a range of white-box attack algorithms and defense mechanisms tailored for deep learning models, such as FGSM [51], DeepFool [52], and C&W [53], which are of significant relevance for assessing the robustness of systems. TextAttack [54], as a testing tool focused on adversarial example generation and model robustness testing for natural language processing tasks, is suitable for white-box attack algorithms like HotFlip [55] and TextFooler [56], providing support for security testing in text-based applications.

Compared to the white-box conditions, model information in the black-box setting is difficult to obtain. Furthermore, black-box attack algorithms can be used to simulate real-world security threats and exploit scenarios, which is crucial for enhancing model robustness. Foolbox [57] is a Python library for generating adversarial samples and evaluating models, which supports various black-box attack algorithms and demonstrates excellent performance across multiple deep learning frameworks such as PyTorch, Keras, and TensorFlow. TextBugger [58] is a black-box adversarial sample generation framework specifically designed for text classification tasks. It can be employed to assess the robustness of deep learning models in text-related tasks. However, the aforementioned DLS testing tools are limited in their applicability as they are designed for specific environments (white-box or black-box) for adversarial robustness evaluation. They do not constitute a universal testing tool and are incapable of effectively assessing model interpretability.

Testing tools for Model Interpretability. Performing interpretability analysis on models is an effective approach to understanding the process by which models generate predictions for different inputs. Moreover, interpretability analysis of models serves as a tool for elucidating the reasons behind errors encountered during DLS testing, thereby enhancing the trustworthiness of models and constituting a vital component of Explainable AI (XAI) research. Presently, several DL testing tools have been developed to elucidate the internal workings and decision processes of DLS, aiming to ensure system quality and reliability. InterpretDL [49] provides a range of functionalities, including feature importance analysis, sample explanations, and model visualization, enabling users to analyze model predictions and gain insights into the underlying patterns and information embedded within the model. NeuronFair [47]addresses reliability and fairness concerns that may arise when applying DNNs in sensitive domains, which serves as a fairness testing framework for building fairer and more trustworthy DLS. However, InterpretDL and NeuronFair often rely on specific DL frameworks, which can be limiting for researchers and practitioners using customized or less common frameworks. In addition, the interpretability of DL models is a complex issue. InterpretDL and NeuronFair do not provide a complete explanation for every decision made by the model, as the effectiveness of model interpretation may be constrained by model complexity. Similarly, the aforementioned methods solely assess the interpretability of DLS, lacking consideration for adversarial robustness.

Testing tools for neuron analysis. A testing tool providing neural analysis utilizes the properties of neurons, including the parameter of each neuron or the performance of each neuron's output under the specific testing input. Many testing tools primarily focus on this aspect. DeepXplore [40] is the first testing tool to propose neural coverage and use the joint optimization method with gradient ascent to generate testing examples. DeepGauge [48] uses neuron states to supervise the purpose of multi-granularity testing coverage. DeepTest [41] uses transformation operations to get higher neural coverage under the specific field of DNN-driven autonomous cars. Although neural coverage is a widely utilized criterion among testing tools, several studies [59], [60] have revealed that relying solely on neural coverage can lead to the generation of misleading testing examples. Overemphasizing neural coverage may result in a limited number of test inputs, potentially overlooking defects in DLS. Based on the premise, Jin *et al.* [61] use shapley value to define excitable neural, which can be regarded as other types of neural analysis. In our research endeavor, we harness the pruning property inherent in DLS, which entails the removal of extraneous neurons from the neural networks through neural analysis. By employing this approach, we aim to discern the intricate relationship between the network's robustness and the presence of indispensable neurons.

3 Preliminaries

In this section, we introduce preliminaries of adversarial attacks, interpretability methods, and neuron pruning methods for evaluating adversarial robustness, model explainability, and model's neuron analysis.

3.1 Adversarial attacks

During the development of ML and DL, DNNs have been proved to have state-of-the-art results in massive fields such as image classification [62], speech recognition [63], natural language processing [64], and recommendation systems [65]. As a multiple-layer unsupervised neural network, the output of DNN is available by layer-to-layer mapping, which can effectively extract the hidden features from the input space and achieve outstanding performance beyond human. Besides, several optimal training methods such as dropout regularization [66] and mini-batching [67] serve to reduce the computation cost of DNNs, allowing the model to have a high prediction accuracy and a fast convergence speed. However, the complex decision boundary of DNNs raises a threat in software quality [68]. Adversarial samples with human-add perturbations as well as noises existed in real-world enable an issue of incorrect model predictions [69]. For example, a DL software system is easily fooled in an image classification task due to its vulnerability towards adversarial samples in the pixel space [70]. The instability of DNNs in the face of adversarial attacks will cause serious security problems, especially in some practical applications that require low false-positive rates (*e.g.,* autonomous driving [71] and cancer detection [72]). It is thus necessary and urgent to explore a deep learning testing tool that can measure the adversarial robustness of DLS.

Nowadays adversarial algorithms are a major approach to test the robustness of models under attack because of the ability to generate promising adversarial samples. Generally, according to the model information that can be accessed, adversarial algorithms can be divided into two categories: white-box attacks [51], [53], [73]–[77] and black-box attacks [78]–[86]. In the white-box environment, the model information(*e.g.,* parameters and structure) can be visited by the attacker. On the contrary, in the black-box environment it is difficult to obtain model details.

White-box adversarial attacks. Gradient-based white-box attacks aim to apply advanced gradient operations to increase the success rate of attack. The FGSM [51] algorithm and some of its derivatives such as I-FGSM [73], MI-FGSM [75], TI-FGSM [76], SINI-FGSM [80], etc. have been proved to have an excellent success rate in the white box model. PGD [74] and C&W [53] algorithms focus on restricting perturbations or using special mathematical constraints to improve the robustness of adversarial examples. In addition, AdvGAN [77] generates adversarial samples by learning a generator network instead of perturbing input samples directly.

Black-box adversarial attacks. As query-based algorithms in black-box attacks, QEBA [78] and ZOO [79] rely on small batches of queries to obtain model information to train adversarial samples. While SSA [84], DIM [81], PIM [82], RAP [87] and NAA [83] are trained on a surrogate model to test the effectiveness of adversarial samples when transferred into the target model.

3.2 Model interpretability

Recently, DNNs remain to be difficult to be interpreted due to the complex hidden layer parameters and incomprehensible nonlinear structure. It is currently unclear how deep models interpret the relationship between their inputs and outputs. Exploring the ambiguous decision-making process of DNNs is an important task in Explainable Artificial Intelligence (XAI) research. For DL software quality testing, a trustworthy system not only needs high accuracy, but also requires to have easy-to-interpret properties in the process of obtaining the results [88]. Therefore, the verification of model interpretability is an important factor for in-depth exploration of the eligibility of DL systems.

To get the corresponding information for the model features and predictions, local approximation methods and gradient based methods are two common directions towards interpreting DNNs. The former attempts to obtain an approximate explanation of the complex target model through a relatively simple and interpretable model, while the latter aims to use the gradient information of the model to obtain the specific relationship between the input features and the outputs.

Local approximation methods. Linear models and decision tree models are widely used in local approximation methods due to the high interpretability of these models [89]–[91]. Other approximation methods add perturbations to training data to obtain the most sensitive part of the inputs with respect to the model outputs [92]–[94].

Gradient based methods. As two early gradient based methods, Grad-CAM [95] and Score-CAM [96] are both class activation mapping (CAM) based methods which aim to explain the relationship between gradient information and intermediate layers of DNN feature maps. Saliency Map [97] (SM) applies gradient directly to obtain the visualisation of the particular features with respect to the model outputs. Guided Backpropagation [98] uses non-negative gradients of the model to get the desired explanation. However, Guided Backpropagation is poorly interpretable for features in negative gradient directions. In addition, only using gradient information is limited for current deep models with increasingly complex structures and diverse application scenarios. For example, SM suffers from gradient saturation and interpretation distortions caused by some noise or changes in external conditions.

To solve the misinterpretation of gradients in specific regions existing in earlier gradient analysis methods, the IG [99] attribution algorithm first extends the original simple gradient calculation into a linear gradient integral from baseline features to input features, improving the interpretability of the model. Introducing prior knowledge as a prior probability distribution for feature attribution, EG [100] has obtained further interpretability improvement on the basis of IG. BIG [101] is firstly proposed to use adversarial attack to determine suitable decision boundaries and apply the attribution method based on IG to find the exact information leading to these decision boundaries. AGI [102] noted that the IG method must seek a specific reference point in the attribution path as a starting point for iteration. In different models, the selection of reference points is complex and unique, which is not conducive to the generalization of IG. Therefore, AGI uses the gradient information of the adversarial sample to integrate along the path with the steepest gradient, so that the contribution of all input features can be calculated without selecting a reference point.

3.3 Algorithm pruning

The initial purpose of the pruning algorithm was to reduce the computational cost of the DL system. The pruning algorithm means preserving valuable parameters in the model while removing redundant parameters [103]. Some work [43], [104] proves that connections between model pruning and robustness exist. From another perspective, the pruning algorithm naturally determines which neuron undertakes the work of model decision-making. As many testing tools have claimed, neural coverage can help increase the quality of testing examples. In order to gain a comprehensive understanding of DLS, it is recommended to employ a pruning algorithm that imposes a stringent constraint on the neurons prior to conducting efficient robustness testing. By implementing pruning techniques, we can alleviate concerns regarding testing methodology bias and focus our efforts on identifying and eliminating redundant parameters.

It is important to note that pruning algorithms can be categorized into two types: those with fine-tuning [105] and those without fine-tuning [106]. Our research specifically concentrates on the design of pruning algorithms without fine-tuning. This choice is motivated by the fact that fine-tuning alters the original parameters, even if it improves performance. Our objective in pruning is to selectively remove certain parameters from DLS while preserving others entirely.

In earlier studies, Hu *et al.* [107] proposed a pruning algorithm to eliminate neurons with zero activation. Subsequently, similar pruning algorithms have placed greater emphasis on the dynamic performance of DLS, such as OBD [108]. OBD employs second-order performance estimation to assess the importance of each neuron. Additionally, Taylor [109] utilizes Taylor expansion to estimate the contribution of individual neurons in decision-making. Greg-2 [110] applies regularization techniques to constrain the estimation of neuron importance, utilizing a clever method to obtain relative importance differences instead of directly calculating the Hessian matrix. OBD, Taylor, Greg-2, and ASL [111] are capable of being executed without the need for fine-tuning, and our work will integrate these approaches.

4 AI-Compass Structure Overview

In this section, we provide a general overview of our work, an all-in-one comprehensive and effective multi-modal testing tool for DLS. The main components of our framework are shown in Figure 1. We aim to develop a framework that exhibits excellent testing performance in both image and text input data, catering to the needs of testing across different modalities. Specifically, we have designed five modules, namely Basic Metrics, Basic Mutants, Robustness Analysis, Interpretability, and Neuron Analysis, to comprehensively test DLS. Within each module, we employ appropriate evaluation metrics to obtain the most reasonable assessment results for the corresponding module. Moreover, we introduce pruning techniques to analyze the redundancy levels of model neurons and investigate the potential alterations in individual modules. This serves as a crucial foundation for optimizing model structure.

It is noteworthy that our framework is an all-in-one solution, serving as a comprehensive, multifunctional, and customizable DLS testing tool. During the preparation stage, diverse DLS undergo two initial collection layers to collect

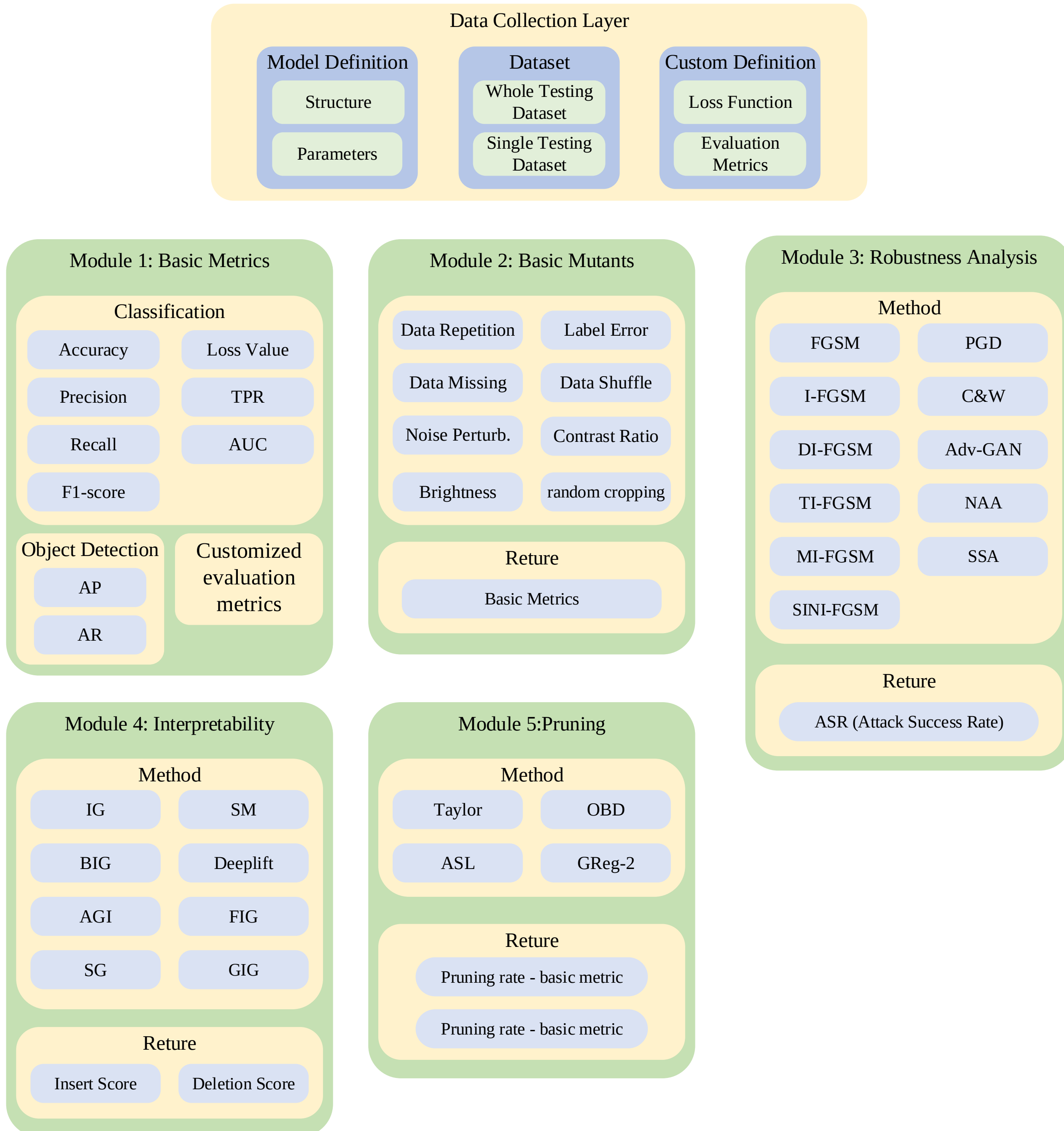

Fig. 1. An overview of AI-COMPASS.

model and dataset information for customizable testing, followed by comprehensive assessment in multiple modules. The visualization of results and the generation of testing reports are provided for researchers or software developers to evaluate the quality of the systems. Users can also customize the testing methods, evaluation techniques, and corresponding metrics based on their specific systems and testing requirements. This ensures the adaptability and flexibility of the testing tool. Table 2 illustrates an overview of the data requirements and supported tasks for each module.

Module 1 Basic Metrics. We employ various fundamental DL evaluation metrics to conduct preliminary testing of DLS. Specifically, for classification tasks, we evaluate the performance using metrics such as accuracy, precision, recall, and loss value. For object detection tasks, we utilize metrics such as average precision (AP) and average recall (AR) to assess the performance.

Module 2 Basic Mutants. We apply various mutant methods such as label error, data repetition, data missing, and noise perturbation to test the specific performance of DLS. The evaluation metrics used in this module are the same as those in Module 1.

Module 3 Robustness Analysis. We employ white-box attack methods such as FGSM [51], PGD [74], and

TABLE 2
Data requirements and supported tasks for each module in the assessment layer of ML-Compass.

Module	Submodule	Single Test Dataset	Whole Test Dataset	Train Dataset	Image Classification	Text Classification	Object Detection
Basic Metrics	Accuracy	○	●	○	●	●	○
	Loss Value	○	●	○	●	●	○
	Precision	○	●	○	●	●	○
	TPR	○	●	○	●	●	○
	Recall	○	●	○	●	●	○
	AUC	○	●	○	●	●	○
	F1-score	○	●	○	●	●	○
	AP	○	●	○	●	●	●
	AR	○	●	○	●	●	●
Basic Mutants	Label Error	●	●	○	●	●	○
	Data Missing	●	●	○	●	●	●
	Data Shuffle	●	●	○	●	●	●
	Noise Perturb	●	●	○	●	●	●
	Contrast Ratio	●	●	○	●	○	●
	Brightness	●	●	○	●	○	●
	Random Cropping	●	●	○	●	○	●
Robustness Analysis	FGSM	●	●	○	●	●	●
	I-FGSM	●	●	○	●	●	●
	DI-FGSM	●	●	○	●	○	●
	TI-FGSM	●	●	○	●	○	●
	MI-FGSM	●	●	○	●	●	●
	SINI-FGSM	●	●	○	●	●	●
	PGD	●	●	○	●	●	●
	C&W	●	●	○	●	○	○
	Adv-GAN	●	●	○	●	○	○
	NAA	●	●	○	●	○	●
	SAA	●	●	○	●	○	●
Interpretability	IG	●	●	○	●	○	○
	BIG	●	●	○	●	○	○
	AGI	●	●	○	●	○	●
	SG	●	●	○	●	○	○
	SM	●	●	○	●	○	○
	Deeplift	●	●	○	●	○	○
	FIG	●	●	○	●	○	●
	GIG	●	●	●	●	○	○
Neuron analysis	Taylor	○	●	●	●	○	○
	ASL	○	●	●	●	○	○
	OBD	○	●	●	●	○	○
	Greg-2	○	●	●	●	○	○

●: the dataset is required (either dataset will fulfill the requirement) or the task is supported; ○: the dataset is not required or the task is not supported.

C&W [53], as well as black-box attack methods including MI-FGSM [75], NAA [83] and SSA [84] to test the robustness of the model against adversarial attacks in both the strongest attack setting and the simulated real-world environment. This enables us to identify and rectify vulnerabilities or loopholes hidden within the system. To effectively evaluate the model's robustness against adversarial attacks, we utilize the attack success rate (ASR) as a benchmark metric in Module 3.

Module 4 Interpretability. In order to understand the intrinsic connection between model outputs and inputs and provide better insights into the decision process at the decision boundary, we employ algorithms such as IG [99], BIG [101], GIG [112], and AGI [102] to obtain model interpretation results. It is worth noting that in Module 4, we employ insertion score and deletion score [113] to evaluate the effectiveness of the model's interpretability.

Module 5 Neuron Analysis. Previous works have demonstrated the remarkable effectiveness of Neuron Analysis in fault detection and localization, optimized test sample generation, and understanding model complexity in DLS testing. Specifically, Neuron Analysis reveals the proportion of effectively utilized neurons, aiding in the discovery of potentially overlooked hidden behaviors or boundary cases, and guiding decisions on model optimization, compression, or pruning. Inspired by this, we integrate state-of-the-art pruning algorithms (*e.g.*, OBD [108], Greg-2 [110], and ASL [111]) into Neuron Analysis Module. These algorithms help analyze the redundancy of model neurons to explore the deep performance of the model and the potential relationships between modules in combination with robustness and interpretability analysis. The Pruning rate serves as the fundamental metric in this module.

5 METHODOLOGY

In this section, we provide a comprehensive technical description of our AI-COMPASS. In the first step, we define and explain the concepts of adversarial attacks and the two attribution axioms. In the second step, we describe the representative methods or algorithms employed in each module. Specifically, in addition to conducting basic metric tests and mutation tests, we comprehensively evaluate model's adversarial robustness by integrating various white-box and black-box adversarial attack algorithms. This approach addresses the limitations of existing testing tools, which are typically confined to either white-box or black-box environments. To provide the most effective explanations for the model's behavior, we incorporate several state-of-the-art attribution algorithms to generate explainable reports for the model. It is worth noting that, for the first time, we have selected several pruning algorithms without fine-tuning as a means of neuron analysis. By testing the pruned model in conjunction with other modules, we analyze the redundancy of the model's neurons and assess its deep performance based on changes in adversarial robustness and model interpretability. For example, if there is no significant change in adversarial robustness or model interpretability after pruning, it can be inferred that the original model contains redundant parameters and has room for further optimization.

5.1 Problem Definition and Invariance Theory

5.1.1 Problem Definition of Adversarial Attack

Formally, suppose we have a deep neural network $N : \mathbb{R}^n \rightarrow \mathbb{R}^c$ and original sample $x \in R^n$. Adversarial attack methods, in this context, are designed to uncover a perturbation denoted as Δx. This perturbation is intended to be added to the original sample x, thereby generating a manipulated input sample denoted as $x' = x + \Delta x$. The overarching objective of the optimization process, in this scenario, is to satisfy the following conditions

$$\min_{x'} D(x, x') \quad \text{subject to} \quad N(x) \neq N(x') \tag{1}$$

We note that for the classification task, $N(x)$ and $N(x')$ should satisfy the constraint as in Equation 1, *i.e.*, $N(x) \neq N(x')$. And for the regression task, the constraint can be defined as $N(x) - N(x') \geq \epsilon$, depending on the application.

5.1.2 Sensitivity and Implementation Invariance

In the context of Integrated Gradients [99] (IG), two crucial concepts are introduced to address the requirements for explaining DNNs: sensitivity and implementation invariance. We believe that these two axioms are of paramount importance in the process of model interpretation.

Sensitivity. Sensitivity pertains to the degree of responsiveness exhibited by an attribution method towards slight perturbations in the input data. In particular, when comparing inputs and baselines that only vary in a single feature but yield different predictions, the attribution method should assign non-zero attributions to the differing features.

Implementation Invariance. Implementation Invariance refers to the attribute of an attribution method that remains unaffected by variations in the implementation of a deep neural network. In formal terms, two networks are considered functionally equivalent if their outputs are equal for all inputs, irrespective of having significantly different implementations. To satisfy Implementation Invariance, attribution methods should consistently produce identical attributions for two functionally equivalent networks.

5.2 Assessment algorithms

5.2.1 Basic & mutant testing

Typically, as a basic module, the fundamental metrics testing exhibits simplicity and provides rapid feedback on test results. We utilize evaluation metrics, as demonstrated in Module 1 of Section 4, to obtain a basic quality estimation of the system. However, recognizing that baseline testing fails to reflect the system's performance under unexpected circumstances, we employ mutation methods in Module 2 to simulate more diverse data distributions and noise scenarios. We consider this as one of the criteria for measuring system stability.

Specifically, in Module 1 and Module 2, it is mandated that the user provides the requisite dataloader for testing purposes. However, a distinction arises between the two modules in terms of the model provision. Module 1 necessitates the user to supply the pre-trained model of their choice, whereas Module 2 does not impose this requirement. Moreover, Module 1 yields the performance metrics values alongside a classification report that is saved as a CSV file. Conversely, Module 2 delivers the dataset after mutant.

5.2.2 Adversarial robustness

As an extension of traditional deep learning system testing, we acknowledge the significance of the system's robustness against adversarial attacks as an indispensable aspect of quality assessment, particularly in the context of privacy and security concerns. In this section, we provide a detailed description of the principles behind the adversarial attack algorithms in Module 3. We present a series of representative algorithms in both white-box and black-box environments. Notably, as shown in Table 1, we innovatively adopt transfer-based attack approaches in the black-box setting to evaluate the model's performance under simulated real-world conditions, which has yet to be proposed in current relevant testing frameworks.

The use of white-box attacks allows for the exploration of a model's robustness when its structure or parameters are potentially exposed, representing a consideration of the worst-case scenario in real-world applications. However, the probability of model parameters or structure leakage in real-life situations is relatively low. Therefore, black-box attacks are more in line with real-world scenarios, where attackers utilize surrogate models to launch attacks on the target model. As a result, we have incorporated a black-box attack testing module, which provides a better evaluation of the model's robustness when its information is not leaked. In general, users have the flexibility to choose whether to provide white-box information, including the model, test sample data, and corresponding labels, or to use black-box models to assess transferability. This choice depends on the specific testing requirements.

FGSM. The Fast Gradient Sign Method (FGSM) is a commonly used white-box adversarial attack algorithm used to generate adversarial samples to deceive DNN models. The formula for FGSM is as follows:

$$x' = x + \epsilon \cdot sign(\nabla_x J(\theta, x, y)) \tag{2}$$

where x' is the generated adversarial sample, ϵ is the hyperparameter that controls the size of the perturbation, $\nabla_x J(\theta, x, y)$ is the gradient of the loss function J with respect to the input x, and sign denotes the sign that takes the gradient.

PGD. Projected Gradient Descent (PGD) is an iterative adversarial attack algorithm which aims to gradually approach an adversarial example by applying small perturbations to the input sample based on gradient information in each iteration. The formulation of the PGD algorithm is as follows:

$$x' = \Pi_{x+S}(x' + \alpha \cdot sign(\nabla_x J(\theta, x', y))) \tag{3}$$

Whereas, α represents the learning rate that controls the step size for each iteration. The Π_{x+S} denotes the projection operation that restricts the perturbed input x' to the valid range defined by $x + S$. $\nabla_x J(\theta, x', y)$ corresponds to the gradient of the loss function J with respect to the input x'; sign signifies taking the sign of the gradient.

MI-FGSM. The Momentum Iterative Fast Gradient Sign Method (MI-FGSM) builds upon the FGSM algorithm by introducing the concept of momentum, which enhances the effectiveness and stability of attacks, particularly in the context of black-box transfer-based attacks.

$$g \leftarrow \mu \cdot g + \frac{\nabla_x J(\theta, x', y)}{|\nabla_x J(\theta, x', y)|} \tag{4}$$

$$x' \leftarrow x' + \alpha \cdot \text{sign}(g) \tag{5}$$

In each iteration, the momentum term g accumulates gradient information and decays based on the momentum factor μ. The introduction of momentum helps maintain a certain level of consistency in the gradient direction during the attack, thereby improving the success rate and stability of transfer-based attacks.

5.2.3 Model interpretability

Currently, the majority of testing tools utilize interpretability methods that focus on specific target class feature maps, such as Grad-CAM [95], lacking a unified and systematic axiomatic discussion. Attribution algorithms based on Integrated Gradients (IG) introduced for the first time two axioms, Sensitivity and Implementation Invariance, which systematically establish a one-to-one correspondence between model outputs and inputs and provide explanations for features that are overlooked by traditional interpretability algorithms. A series of algorithms, including BIG and AGI, are dedicated to optimizing the potential drawbacks of IG to further enhance the accuracy of attributions.

By comparing various interpretability methods, users can assess the model's interpretability capability. Specifically, by evaluating multiple instances of the same interpretability method, a model demonstrating superior evaluation metrics indicates better interpretability. This signifies a higher level of trustworthiness in the model. In this section, we primarily introduce attribution algorithms represented by IG and its variants to conduct a generic assessment of model interpretability.

IG. As mentioned in 5.1.2, IG proposed two axiomatic criteria: *Sensitivity* and *Implementation Invariance*. By carefully selecting reference points as anchors along a linear integration path, IG effectively integrates the continuous gradients to determine the attribution of individual input features. The formula of IG is expressed in Equation 6.

$$IG_j(x) = (x_j - x'_j) \times \int_{\alpha=0}^{1} \frac{\partial F(x' + \alpha \times (x - x'))}{\partial x_j} \mathrm{d}\alpha \tag{6}$$

where j denotes the j-th input feature, $\frac{\partial F(x'+\alpha\times(x-x'))}{\partial x_j}$ is the gradient of model F w.r.t input feature x_j. x'_j represents the reference input feature.

BIG. Through investigating improved baseline selection techniques in comparison to IG, the Boundary-based Integrated Gradient (BIG) method introduces boundary search to achieve more precise attribution outcomes. Considering a deep learning network F, the Integrated Gradient g_{IG}, and an input feature x, the formula is expressed as Equation 7.

$$B_{\mathrm{IG}}(\mathbf{x}) := g_{\mathrm{IG}}(\mathbf{x}; \mathbf{x}') \tag{7}$$

where x' is the nearest adversarial example to x, *i.e.*, $c = F(x) \neq F(x')$ and $\forall \mathbf{x}_m \cdot \|\mathbf{x}_m - \mathbf{x}\| < \|\mathbf{x}' - \mathbf{x}\| \rightarrow F(\mathbf{x}) = F(\mathbf{x_m})$.

AGI. The Adversarial Gradient Integration (AGI) method aims to identify the steepest non-linear ascending path from the adversarial example x'_i to x, eliminating the requirement for reference points along the path, unlike IG. The formula is defined as Equation 8 in the following:

$$AGI_j(x) = AGI_{j-1}(x) - \nabla_{x_j} f^t(x) \cdot \epsilon \cdot sign(\frac{\nabla_{x_j} f^i(x)}{|\nabla_{x_j} f^i(x)|}) \tag{8}$$

$\nabla_{x_j} f^t(x)$ represents the gradient of the output value $f^t(x)$ w.r.t the j-th input feature x, where t denotes the true class label. Similarly, $\nabla_{x_j} f^i(x)$ represents the gradient corresponding to the false class label i. The step size is denoted by ϵ. The integration process continues along the path until $argmax_l f^l(x) = i$, indicating that the attribution integration stops when the predicted class label becomes i.

To conduct interpretability analysis, the user is required to provide the model, the test data along with its corresponding labels. By utilizing the aforementioned interpretability algorithms, the user can obtain the interpretability heat map or attribution map for a single image, as well as the average insertion and deletion scores for multiple test samples.

5.2.4 Neuron analysis

In this section, we introduce for the first time the integration of pruning methods into our testing tool. By pruning model parameters at a certain proportion, we observe the performance changes. If the performance changes are small or within an acceptable range, it indicates that the pruned parameters are redundant. Hence, pruning algorithms can be used to evaluate model redundancy.

Furthermore, models with excessive redundancy are susceptible to the risk of overfitting. By employing different pruning rates and methods, we investigate the robustness and interpretability of the model under various conditions. This assists users in selecting models that better meet their requirements without the need for retraining, while minimizing significant performance changes.

We compare the changes in ASR and Insertion & Deletion Score [102] before and after employing pruning algorithms, examining the impact of pruning on the modules of adversarial robustness and model interpretability. Furthermore, we proceed to introduce several representative pruning algorithms.

OBD. The Optimal Brain Damage (OBD) algorithm employs a second-order expansion technique to estimate the performance of DLS by considering the impact of removing specific neurons.

$$\delta E = \frac{1}{2} \sum_i h_{ii} \delta u_i^2 \tag{9}$$

where h_{ii} represents the Hessian matrix and δu_i^2 denotes the value associated with the i-th neuron, OBD allows for the pruning of neurons with minimal perturbation to the overall error (δE). In OBD, the calculation of the Hessian matrix is approximated to streamline the process. Typically, neurons exhibiting lower δE are considered non-essential for the proper functioning of DLS.

Taylor. The Taylor algorithm leverages a combination of regularization techniques and Taylor expansion to estimate the significance of neurons within a neural network.

$$\delta E(u) = (g_m \delta u_i)^2 \tag{10}$$

where δu_i is the value of i-th neuron, g_m is the gradient value under the regularization. δE is simplified to use the first-order expansion for computational optimization.

Greg-2. Greg-2 algorithm takes into account the importance of neurons in a dynamic and relative context. It eliminates the need to compute the Hessian matrix during the pruning process by considering the relative relationships between neurons. For a more comprehensive understanding of Greg-2 and another algorithm called ASL, please refer to the references [110] and [111].

In summary, the Pruning module requires the provision of the test model, train dataset, test dataset, and the desired pruning scale by the user. Upon completion, the pruned model is returned, along with performance metrics such as accuracy before and after the pruning process.

6 Experiment Setup

6.1 Experimental Environment

The present tool is developed on PyTorch 1.11. All experiments conducted in this study are performed on a server running Ubuntu 20.04.4, equipped with AMD EPYC 7642 48-Core Processor, NVIDIA RTX3090 GPU, and 80GB RAM.

6.2 Datasets

In this study, we employed several well-known datasets from the domains of image classification, object detection, and text classification. Specifically, for the image classification task, the CIFAR-100 dataset [114] was utilized. The COCO dataset [115] was employed for the object detection domain. As for the text classification task, we utilized the STT-2 dataset [116].

6.3 Models

In this experiment, in order to demonstrate the comprehensiveness and effectiveness of our testing framework, we conducted three different categories of tasks: image classification, object detection, and text classification, within each module. Additionally, for each task, we tested two different models to examine the performance differences between them. We use ResNet-50 [1] and VGG-16 [2] for image classification tasks, TextCNN [117] and AB-LSTM [118] for text classification tasks, Faster R-CNN [119] and RetinaNet [120] for object detection tasks.

6.4 Metrics

In our evaluation part, in addition to the basic and commonly used metrics mentioned in Module 1, such as accuracy, recall, precision, etc., we have also included additional metrics in the extended modules to provide a more comprehensive assessment of DLS performance.

Regarding the evaluation of model robustness, we utilized the Attack Success Rate (ASR), which represents the proportion of successful adversarial samples in the total number of attack samples. Thus, it can be used to evaluate the performance of an attack method on a specific model.

In terms of evaluating model interpretability, we introduced the concept of interpretability analysis for individual data samples and multiple data samples. For the former, analysis is conducted by examining the heatmaps returned by the evaluation framework, which utilize different colors to assess the accuracy of the DLS system in capturing salient features. In the case of multiple samples, we employed the Insertion score and Deletion score [113] for evaluation. The Insertion score involves starting with an empty image and progressively adding pixels based on their attribution scores, beginning with the highest score and moving towards the lowest. Similarly, the Deletion score is obtained by iteratively removing pixels from the original image in descending order of their attribution scores.

In the neural analysis of DLS, we employed the pruning rate as our evaluation metric, which represents the proportion of parameters pruned from the model out of the total model parameters.

TABLE 3
The results of basic metrics and mutant testing.

Model	Method	Accuracy	Loss Value	TPR	TNR	PPV	NPV	FPR	FNR	FDR	ROC_AUC	Precision	Recall	F1-Score
ResNet-50	Origin Image	0.7929	3.8597	0.7929	0.9979	0.7936	0.9979	0.0021	0.2071	0.2064	0.9902	0.7936	0.7929	0.7922
	Label Error	0.7128	3.9354	0.7133	0.9971	0.7137	0.9971	0.0029	0.2867	0.2863	0.9402	0.7137	0.7133	0.7121
	Data Missing	0.5893	4.0795	0.5893	0.9959	0.6854	0.9959	0.0041	0.4107	0.3146	0.9608	0.6854	0.5893	0.6013
	Data Shuffle	0.7929	3.8597	0.7929	0.9979	0.7936	0.9979	0.0021	0.2071	0.2064	0.9902	0.7936	0.7929	0.7922
	Noise Perturb	0.3796	4.2737	0.3796	0.9937	0.6011	0.9937	0.0063	0.6204	0.3989	0.8871	0.6011	0.3796	0.4047
	Contrast Ratio	0.7884	3.8649	0.7884	0.9979	0.7888	0.9979	0.0021	0.2116	0.2112	0.9898	0.7888	0.7884	0.7876
	Brightness	0.7883	3.8646	0.7883	0.9979	0.789	0.9979	0.0021	0.2117	0.211	0.9897	0.789	0.7883	0.7875
	Random Cropping	0.7391	3.9369	0.7391	0.9974	0.7441	0.9974	0.0026	0.2609	0.2559	0.9863	0.7441	0.7391	0.7388
VGG-16	Origin Image	0.7259	3.91	0.7259	0.9972	0.7275	0.9972	0.0028	0.2741	0.2725	0.9855	0.7275	0.7259	0.7254
	Label Error	0.6525	3.9821	0.653	0.9965	0.6543	0.9965	0.0035	0.347	0.3457	0.9363	0.6543	0.653	0.652
	Data Missing	0.5163	4.1185	0.5163	0.9951	0.5698	0.9951	0.0049	0.4837	0.4302	0.9486	0.5698	0.5163	0.5135
	Data Shuffle	0.7259	3.91	0.7259	0.9972	0.7275	0.9972	0.0028	0.2741	0.2725	0.9855	0.7275	0.7259	0.7254
	Noise Perturb	0.3966	4.237	0.3966	0.9939	0.5388	0.9939	0.0061	0.6034	0.4612	0.9024	0.5388	0.3966	0.4138
	Contrast Ratio	0.7182	3.9164	0.7182	0.9972	0.7198	0.9972	0.0028	0.2818	0.2802	0.985	0.7198	0.7182	0.7175
	Brightness	0.7223	3.9152	0.7223	0.9972	0.7236	0.9972	0.0028	0.2777	0.2764	0.9849	0.7236	0.7223	0.7217
	Random Cropping	0.648	3.9879	0.648	0.9964	0.6614	0.9964	0.0036	0.352	0.3386	0.9768	0.6614	0.648	0.6494

6.5 Parameter Setting

In this experiment, apart from the pruning rate, all other parameter settings followed the default parameters specified in the original method. Users have the flexibility to customize these parameters for their subsequent usage. As for the pruning rate parameter, we set it to 0.35, 0.4, 0.45, and 0.5, respectively.

6.6 Research questions

In our experimental study, we aim to investigate and address the following research questions:

- **RQ1:** Does AI-COMPASS effectively integrate each module so as to provide a comprehensive assessment of the model's performance?
- **RQ2:** In addition to image classification tasks, does AI-COMPASS meet the test requirements under other modal tasks such as text classification and object detection? Does it overcome the shortcoming of ad-hoc in existing testing tools?
- **RQ3:** Combining the Adversarial Robustness and Model Interpretability modules, can AI-COMPASS use the pruning method to evaluate model depth performance and give optimization recommendations?

7 EXPERIMENTAL RESULTS

7.1 Answer to RQ1

In this section, we performed basic utility evaluation, robustness evaluation, interpretability analysis and neuron analysis with pruning to verify which model in each module shows superior performance.

7.1.1 Basic utility evaluation

As shown in Table 3, considering all the metrics collectively, it can be observed that under various data processing methods such as the original dataset, label errors, missing data, and shuffled data, ResNet-50 slightly outperforms VGG-16 with higher accuracy and lower loss values in these scenarios, indicating its superior performance and generalization capability in handling such data.

However, under the data processing method involving noise perturbation, VGG-16 exhibits a slight advantage over ResNet-50. Although VGG-16 achieves a slightly higher accuracy compared to ResNet-50, the difference between the two models is not statistically significant.

Therefore, taking into account the performance across different data processing methods, it can be concluded that ResNet-50 and VGG-16 perform comparably overall, but in most cases, ResNet-50 demonstrates slightly better performance than VGG-16.

7.1.2 Robustness evaluation

In the experiment of this module, we employed two different types of attack methods: white-box attacks and black-box attacks. As shown in Table 4, for white-box attacks, VGG-16 demonstrates a lower ASR compared to ResNet-50. Therefore, on the dataset used in this experiment, VGG-16 exhibits better robustness than ResNet-50. Considering the practical application scenarios of DLS, we incorporated transfer-based black-box attacks to simulate real-world testing conditions. In the black-box attacks, VGG-16 consistently achieves a lower ASR than ResNet-50, indicating it has better robustness than ResNet-50 in this particular task.

7.1.3 Interpretability analysis

In the experiments conducted in this module, we initially performed a global assessment of model interpretability using the Insertion Score and Deletion Score. As shown in Table 5, we observed that ResNet-50 exhibits relatively higher Insertion Score and lower Deletion Score compared to VGG-16, indicating that ResNet-50 possesses better interpretability. Furthermore, based on Table 5, we found that the AGI, BIG, and Saliency Map methods demonstrate relatively good attribution performance on both ResNet-50 and VGG-16. Therefore, we analyzed the heatmaps generated by these three methods for further analysis. As shown in Figure 2, the white regions in the heatmaps represent the features that the model focuses on. From the top-left corner, which displays the original image, it can be observed that ResNet-50 exhibits a more concentrated focus on specific features compared to VGG-16, thus demonstrating better interpretability.

7.1.4 Neuron analysis with pruning

The purpose of this experiment is to evaluate the impact of different pruning rates on the performance of ResNet-50

TABLE 4
Table of model robustness evaluation results, the data in the table are ASR, the bolded data are the results of white box attack, the unbolded data are the results of black box attack.

Test Model	Attack Method	ResNet-50	VGG-16	Inception-v3	DenseNet-121	GoogLeNet	MobileNet-v2
ResNet-50	FGSM	79.11%	58.34%	69.14%	68.74%	66.59%	57.54%
	I-FGSM	99.97%	53.25%	75.42%	75.20%	66.01%	44.57%
	DI-FGSM	99.72%	67.30%	84.06%	83.93%	79.46%	63.88%
	TI-FGSM	86.49%	22.66%	36.56%	30.84%	30.48%	22.30%
	MI-FGSM	99.87%	64.47%	80.98%	81.33%	75.23%	56.99%
	SINI-FGSM	98.37%	60.63%	76.23%	74.98%	69.82%	57.78%
	PGD	99.99%	53.31%	74.21%	74.37%	64.93%	44.08%
	C&W	80.50%	6.57%	13.42%	14.49%	9.27%	4.12%
	Adv-GAN	87.83%	86.18%	83.86%	79.93%	81.83%	52.05%
	NAA	91.65%	70.61%	84.06%	64.99%	75.53%	65.04%
	SSA	97.00%	60.27%	93.38%	91.88%	80.19%	57.67%
	Average	**92.77%**	**54.87%**	**70.12%**	**67.33%**	**63.58%**	**47.82%**
VGG-16	FGSM	57.99%	75.81%	63.35%	62.25%	62.49%	54.52%
	I-FGSM	44.04%	99.17%	59.93%	56.05%	55.45%	40.21%
	DI-FGSM	69.64%	97.49%	76.09%	73.65%	75.17%	63.54%
	TI-FGSM	41.76%	91.96%	43.40%	37.59%	39.79%	31.36%
	MI-FGSM	60.87%	98.51%	71.18%	68.33%	67.85%	53.33%
	SINI-FGSM	59.41%	94.88%	66.42%	62.93%	62.53%	54.60%
	PGD	41.24%	99.16%	57.84%	52.51%	52.56%	35.77%
	C&W	6.71%	68.20%	7.38%	7.56%	7.56%	3.69%
	Adv-GAN	40.26%	91.03%	71.01%	55.58%	79.19%	36.10%
	NAA	62.27%	98.68%	74.33%	53.03%	67.52%	61.39%
	SSA	57.37%	90.40%	84.63%	79.85%	69.88%	50.62%
	Average	**49.23%**	**91.39%**	**61.41%**	**55.39%**	**58.18%**	**44.10%**

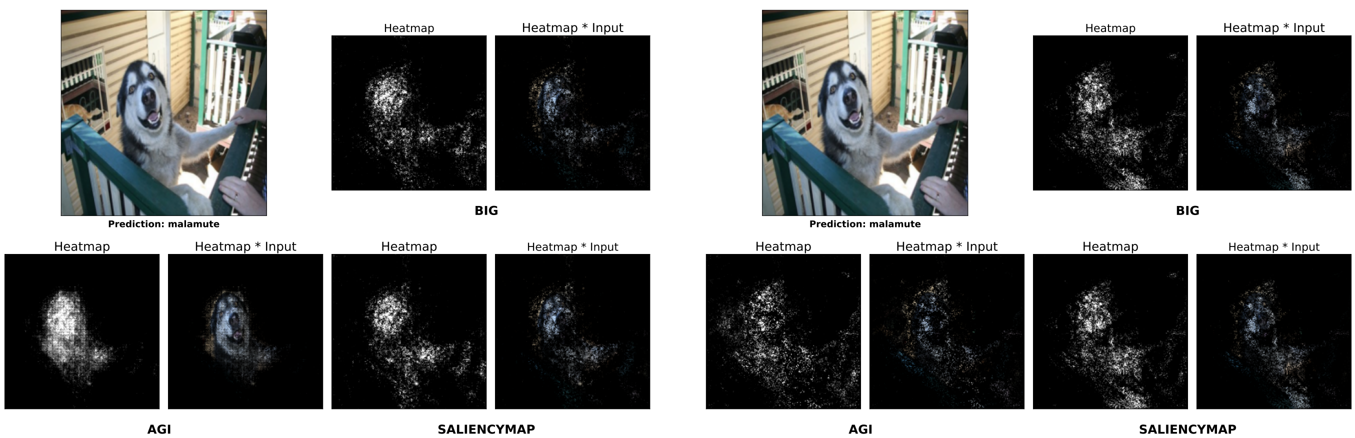

(a) ResNet-50 Interpretability Result

(b) VGG-16 Interpretability Result

Fig. 2. Attribution Results of the Models

and VGG-16 models. We employed four different pruning methods, including Taylor, ASL, OBD, and Greg-2, and observed the performance variations at different pruning rates. Firstly, we recorded the baseline performance of both models without pruning: ResNet-50 achieved an accuracy of 0.7929 and a loss value of 3.8597, while VGG-16 achieved an accuracy of 0.7259 and a loss value of 3.91.

Next, we conducted pruning experiments with different pruning rates and recorded the changes in performance metrics. In the ResNet-50 model, using the Taylor pruning method, when the pruning rate was set to 0.35, the accuracy dropped to 0.7301, and the loss value increased to 3.9557. As the pruning rate increased, the accuracy further declined, and the loss value continued to increase. When the pruning rate reached 0.5, the accuracy sharply dropped to 0.0554, and the loss value increased to 4.5603. In the VGG-16 model, using the Taylor pruning method, the accuracy gradually decreased and the loss value increased as the pruning rate increased. At a pruning rate of 0.5, the accuracy was 0.7175, and the loss value was 3.9317.

In addition to the Taylor pruning method, we also investigated the impact of ASL, OBD, and Greg-2 pruning methods on performance. For the ResNet-50 model, with ASL and OBD pruning methods, the accuracy gradually decreased as the pruning rate increased, while with the Greg-2 pruning method, the accuracy remained relatively stable, indicating a minor impact of pruning rate on performance. For the VGG-16 model, with ASL and OBD pruning methods, the accuracy gradually decreased as the pruning rate increased. While with the Greg-2 pruning method, similar to the ResNet-50 model, the accuracy remained relatively stable, indicating a minor impact of pruning rate

TABLE 5
Insertion and Deletion Score of ResNet-50 and VGG-16

Model	Method	Insertion Score	Deletion Score
ResNet-50	IG	0.1136	0.0246
	BIG	0.2272	0.042
	AGI	0.3881	0.0463
	SG	0.2352	0.0197
	SM	0.1242	0.0332
	DeepLIFT	0.1246	0.0256
	FIG	0.0889	0.0314
	GIG	0.1267	0.0186
	SaliencyMap	0.2559	0.0479
	Average	0.1872	0.0321
VGG-16	IG	0.0804	0.02
	BIG	0.1828	0.0316
	AGI	0.3428	0.0393
	SG	0.1343	0.0162
	SM	0.0834	0.0242
	DeepLIFT	0.0956	0.0182
	FIG	0.0682	0.0244
	GIG	0.0906	0.0165
	SaliencyMap	0.2279	0.0336
	Average	0.1451	0.0249

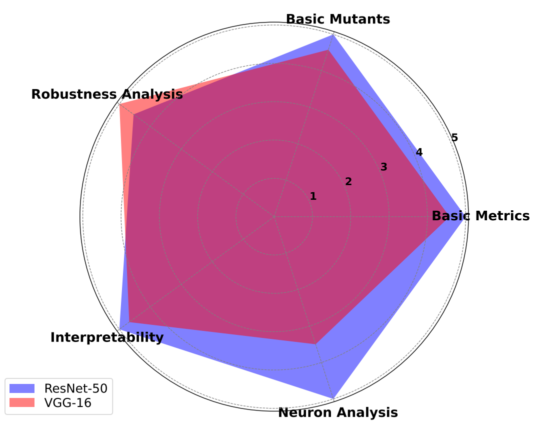

Fig. 3. Comprehensive Evaluation Result

on performance.

In summary, compared to VGG-16, ResNet-50 exhibits more pronounced performance fluctuations under the same pruning rate, indicating a larger proportion of critical parameters within the ResNet-50 model. This observation suggests that the neurons in ResNet-50 possess a lower degree of redundancy. As a deep residual network, ResNet-50 preserves more essential and refined data through skip connections and residual blocks, rendering it more susceptible to the effects of pruning methods. In contrast, VGG-16 adheres to a more traditional convolutional neural network architecture, potentially incorporating more redundant structures, which imparts greater tolerance to neuron pruning.

7.1.5 Comprehensive Evaluation

Our approach allows for a comprehensive evaluation of models, enabling users to intuitively assess the performance of different competing models across five distinct modules. As depicted in Figure 3, users can customize their selection

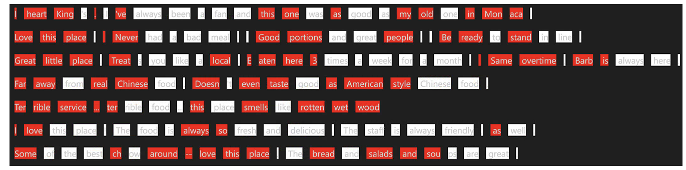

Fig. 4. Interpretability of the text classification model.

of evaluation metrics for scoring sub-modules based on the emphasis of different tasks. In this particular example, we chose Precision as the evaluation metric in the Basic Metrics module, Precision under Label Error conditions in the Basic Mutants module, Average ASR of all attack methods in the Robustness Analysis module, Average Insertion Score in the Interpretability module, and in the Neural Analysis module, we select the maximum pruning rate that maintains model performance as our evaluation metric. We define the best model performance in the test set as a full score of 5 points, while other models are scored proportionally. Through this comprehensive assessment, it becomes evident that the ResNet-50 model outperforms the VGG-16 model across all aspects, except for Robustness.

7.2 Answer to RQ2

In this section, we demonstrate that the aforementioned modules support multimodal data, offering support for both text classification tasks and object detection tasks. We present the experimental results of AI-Compass for these two tasks, showcasing its superior performance.

7.2.1 Performance in text classification tasks

As depicted in Table 7, we present the evaluation of text classification models. The evaluation is conducted on TextCNN and AB-LSTM models using the SST-2 dataset. It can be observed that both models exhibit remarkably similar performance across most metrics. However, AB-LSTM outperforms TextCNN marginally in certain metrics such as Loss Value, Positive Predictive Value (PPV), Negative Predictive Value (NPV), False Positive Rate (FPR), False Negative Rate (FNR), and False Discovery Rate (FDR). Therefore, it can be inferred that the AB-LSTM model demonstrates slightly superior performance compared to the TextCNN model in this task.

As presented in Table 8, the data generated by the Robustness module for testing text classification models is displayed. Based on the data in the table, we can observe that the AB-LSTM model demonstrates higher Attack Success Rates (ASR) under FGSM, SINI-FGSM, and PGD attacks. Conversely, the TextCNN model exhibits higher ASR under I-FGSM and MI-FGSM attacks. In general, the TextCNN model demonstrates a stable robustness, with a comparable defense performance across each attack method. On the other hand, the AB-LSTM model exhibits strong defense capabilities against certain attack methods while displaying weaker defense against others.

Figure 4 showcases the output results of the interpretability module for text classification tasks, wherein darker colors indicate a higher degree of model attention towards the corresponding regions of interest.

TABLE 6
Results of Utility evaluation of pruning models.

Model	Method	Pruning Rate	Accuracy	Loss Value	TPR	TNR	PPV	NPV	FPR	FNR	FDR	ROC_AUC	Precision	Recall	F1-Score
ResNet-50	No pruning	0	0.7929	3.8597	0.7929	0.9979	0.7936	0.9979	0.0021	0.2071	0.2064	0.9902	0.7936	0.7929	0.7922
	Taylor	0.35	0.7301	3.9557	0.7301	0.9973	0.7721	0.9973	0.0027	0.2699	0.2279	0.9877	0.7721	0.7301	0.7367
		0.4	0.6112	4.0869	0.6112	0.9961	0.817	0.9961	0.0039	0.3888	0.183	0.9798	0.817	0.6112	0.6602
		0.45	0.3058	4.3593	0.3058	0.993	N/A	0.993	0.007	0.6942	N/A	0.9313	0.8389	0.3058	0.3847
		0.5	0.0554	4.5603	0.0554	0.9905	N/A	0.9906	0.0095	0.9446	N/A	0.8338	0.3402	0.0554	0.0614
	ASL	0.35	0.6257	4.0277	0.6257	0.9962	0.7221	0.9962	0.0038	0.3743	0.2779	0.9717	0.7221	0.6257	0.6017
		0.4	0.5566	4.0994	0.5566	0.9955	0.7046	0.9955	0.0045	0.4434	0.2954	0.9608	0.7046	0.5566	0.5148
		0.45	0.5412	4.1178	0.5412	0.9954	N/A	0.9954	0.0046	0.4588	N/A	0.959	0.6716	0.5412	0.4821
		0.5	0.4944	4.1717	0.4944	0.9949	N/A	0.9949	0.0051	0.5056	N/A	0.953	0.5922	0.4944	0.4344
	OBD	0.35	0.7393	4.0965	0.7393	0.9974	0.7865	0.9974	0.0026	0.2607	0.2135	0.9898	0.7865	0.7393	0.7434
		0.4	0.6293	4.2932	0.6293	0.9963	0.8092	0.9963	0.0037	0.3707	0.1908	0.9886	0.8092	0.6293	0.6514
		0.45	0.4372	4.4456	0.4372	0.9943	N/A	0.9944	0.0057	0.5628	N/A	0.9873	0.8244	0.4372	0.4691
		0.5	0.2719	4.5201	0.2719	0.9926	N/A	0.9927	0.0074	0.7281	N/A	0.9851	0.6469	0.2719	0.281
	Greg-2	0.35	0.7879	3.866	0.7879	0.9979	0.7894	0.9979	0.0021	0.2121	0.2106	0.9903	0.7894	0.7879	0.7871
		0.4	0.7873	3.8704	0.7873	0.9979	0.7892	0.9979	0.0021	0.2127	0.2108	0.9903	0.7892	0.7873	0.7865
		0.45	0.7852	3.8768	0.7852	0.9978	0.7879	0.9978	0.0022	0.2148	0.2121	0.9902	0.7879	0.7852	0.7844
		0.5	0.7785	3.8882	0.7785	0.9978	0.7823	0.9978	0.0022	0.2215	0.2177	0.9901	0.7823	0.7785	0.7776
VGG-16	No pruning	0	0.7259	3.91	0.7259	0.9972	0.7275	0.9972	0.0028	0.2741	0.2725	0.9855	0.7275	0.7259	0.7254
	Taylor	0.35	0.725	3.9109	0.725	0.9972	0.7266	0.9972	0.0028	0.275	0.2734	0.9852	0.7266	0.725	0.7247
		0.4	0.7243	3.9132	0.7243	0.9972	0.7259	0.9972	0.0028	0.2757	0.2741	0.9849	0.7259	0.7243	0.724
		0.45	0.7218	3.9187	0.7218	0.9972	0.7254	0.9972	0.0028	0.2782	0.2746	0.9843	0.7254	0.7218	0.7221
		0.5	0.7175	3.9317	0.7175	0.9971	0.726	0.9971	0.0029	0.2825	0.274	0.9829	0.726	0.7175	0.7186
	ASL	0.35	0.6585	3.9793	0.6585	0.9966	0.6773	0.9966	0.0034	0.3415	0.3227	0.9738	0.6773	0.6585	0.6562
		0.4	0.6255	4.0125	0.6255	0.9962	0.6555	0.9962	0.0038	0.3745	0.3445	0.9682	0.6555	0.6255	0.6225
		0.45	0.5786	4.0637	0.5786	0.9957	0.6319	0.9957	0.0043	0.4214	0.3681	0.9594	0.6319	0.5786	0.5766
		0.5	0.5435	4.1002	0.5435	0.9954	0.6168	0.9954	0.0046	0.4565	0.3832	0.9529	0.6168	0.5435	0.5413
	OBD	0.35	0.7262	3.9106	0.7262	0.9972	0.7277	0.9972	0.0028	0.2738	0.2723	0.9855	0.7277	0.7262	0.7256
		0.4	0.7259	3.9116	0.7259	0.9972	0.7275	0.9972	0.0028	0.2741	0.2725	0.9854	0.7275	0.7259	0.7253
		0.45	0.7264	3.9135	0.7264	0.9972	0.7281	0.9972	0.0028	0.2736	0.2719	0.9853	0.7281	0.7264	0.7259
		0.5	0.7261	3.917	0.7261	0.9972	0.7282	0.9972	0.0028	0.2739	0.2718	0.9852	0.7282	0.7261	0.7257
	Greg-2	0.35	0.723	3.912	0.723	0.9972	0.7248	0.9972	0.0028	0.277	0.2752	0.9859	0.7248	0.723	0.722
		0.4	0.721	3.9159	0.721	0.9972	0.7241	0.9972	0.0028	0.279	0.2759	0.9855	0.7241	0.721	0.7201
		0.45	0.7148	3.9204	0.7148	0.9971	0.7175	0.9971	0.0029	0.2852	0.2825	0.9851	0.7175	0.7148	0.7133
		0.5	0.7091	3.9281	0.7091	0.9971	0.7133	0.9971	0.0029	0.2909	0.2867	0.9844	0.7133	0.7091	0.7068

TABLE 7
The results of basic metrics and mutant testing of the text classification

Task	Dataset	Model	Method	Accuracy	Loss Value	TPR	TNR	PPV	NPV	FPR	FNR	FDR	ROC_AUC	Precision	Recall	F1-Score
Text Classification	SST-2	TextCNN	Origin Image	0.84	0.4674	0.84	0.84	0.8401	0.8401	0.16	0.16	0.1599	0.9235	0.8401	0.84	0.84
			Label Error	0.7727	0.5299	0.7727	0.7727	0.7727	0.7727	0.2273	0.2273	0.2273	0.8383	0.7727	0.7727	0.7727
			Data Missing	0.8222	0.4828	0.8222	0.8222	0.8223	0.8223	0.1778	0.1778	0.1777	0.9092	0.8223	0.8222	0.8222
			Data Shuffle	0.84	0.4674	0.84	0.84	0.8401	0.8401	0.16	0.16	0.1599	0.9235	0.8401	0.84	0.84
		AB-LSTM	Origin Image	0.8406	0.4645	0.8406	0.8406	0.8407	0.8407	0.1594	0.1594	0.1593	0.9212	0.8407	0.8406	0.8406
			Label Error	0.7664	0.5322	0.7666	0.7666	0.7665	0.7665	0.2334	0.2334	0.2335	0.8355	0.7665	0.7666	0.7664
			Data Missing	0.8228	0.4798	0.8228	0.8228	0.8228	0.8228	0.1772	0.1772	0.1772	0.9053	0.8228	0.8228	0.8228
			Data Shuffle	0.8406	0.4645	0.8406	0.8406	0.8407	0.8407	0.1594	0.1594	0.1593	0.9212	0.8407	0.8406	0.8406

TABLE 8
Table of model robustness evaluation results, the data in the table are ASR

Task	Dataset	Model	Method	ASR
Text Classification	SST-2	TextCNN	FGSM	86.60%
			I-FGSM	85.80%
			MI-FGSM	86.50%
			SINI-FGSM	79.10%
			PGD	86.40%
		AB-LSTM	FGSM	97.70%
			I-FGSM	75.60%
			MI-FGSM	48.90%
			SINI-FGSM	94.80%
			PGD	99.80%

7.2.2 *Performance in object detection tasks*

Table 9 presents the evaluation of object detection tasks. In this section, the performance of Faster R-CNN and RetinaNet models was assessed using the COCO dataset. Both models exhibited relatively similar performance across different metrics. However, Faster R-CNN demonstrated a slight advantage in terms of overall average precision, while RetinaNet showcased a slight advantage in terms of overall average recall.

Table 10 presents the robustness evaluation of the object detection task. From the data, it can be observed that RetinaNet exhibits better robustness than Faster R-CNN, as it maintains higher average precision and average recall even after undergoing the same attacks. This indicates that RetinaNet demonstrates stronger resilience against attacks compared to Faster R-CNN.

7.3 Answer of RQ3

By combining the Adversarial Robustness and Model Interpretability modules in AI-COMPASS, we utilize pruning techniques to evaluate the performance of the model and provide optimization advice. Thus, the model complexity is reduced whilst the generalization ability is enhanced [121]. We have further investigated the impact of the pruning algorithm on model performance by combining the pruning results with the robustness and interpretability analysis.

TABLE 9
The results of basic metrics and mutant testing of the object detection

Task	Dataset	Model	Method	AP	AR
Object detection	COCO	Faster R-CNN	Origin Image	0.585	0.508
			Data Missing	0.08	0.106
			Data Shuffle	0.585	0.508
			Noise Perturb	0.422	0.391
			Contrast Ratio	0.581	0.506
			Brightness	0.579	0.506
			Random Cropping	0.548	0.433
		RetinaNet	Origin image	0.557	0.537
			Data Missing	0.081	0.157
			Data Shuffle	0.557	0.537
			Noise Perturb	0.394	0.424
			Contrast Ratio	0.554	0.535
			Brightness	0.553	0.535
			Random Cropping	0.523	0.461

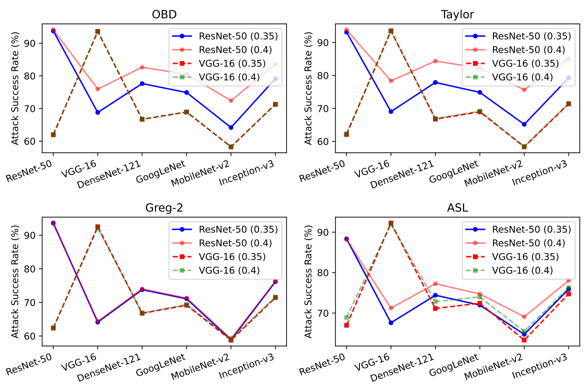

Fig. 5. Average Attack Success Rate with different Pruning Rate

7.3.1 *The impact of pruning on adversarial robustness*

As depicted in Figure 5, we applied four different pruning algorithms to perform parameter pruning on ResNet-50 and VGG-16, achieving pruning ratios of 35% and 40% respectively. Observations indicate that, on the whole, VGG-16 exhibits superior robustness compared to ResNet-50. Following the pruning process, the robustness of VGG-16 remained almost unchanged, while ResNet-50 experienced a relatively substantial performance decline. Additionally, we noted that pruning the model using the Greg-2 method had minimal impact on the model's robustness.

7.3.2 *The impact of pruning on model Interpretability*

As shown in Figure 6, we applied four different pruning algorithms to prune ResNet-50 and VGG-16 models by 35% and 40% respectively. It can be observed that compared to ResNet-50, VGG-16 exhibits a higher Insertion Score. However, the increase in Deletion Score for VGG-16 compared to ResNet-50 is only marginal. This suggests that in this experiment, VGG-16 demonstrates better interpretability than ResNet-50. It is worth noting that when using the Taylor method for pruning, ResNet-50 shows a sharp increase in Deletion Score, which could indicate that ResNet-50 is approaching its pruning limit. Additionally, when using the ASL pruning method, VGG-16 outperforms ResNet-50 in both Insertion Score and Deletion Score, indicating that VGG-16 exhibits superior interpretability across all aspects compared to ResNet-50 at this particular pruning stage.

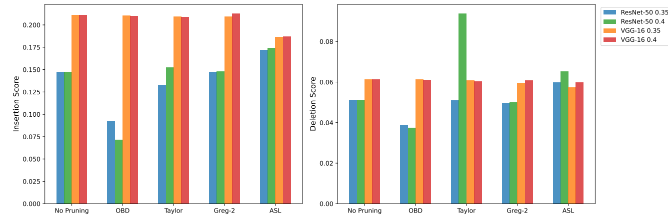

Fig. 6. Average Insertion Score and Deletion Score with Different Pruning Rate. A higher Insertion Score indicates better model interpretability, while a lower Deletion Score indicates better interpretability. The comparison between Insertion Score and Deletion Score reflects the model's overall interpretability strength.

8 Conclusion

In this paper, we proposed AI-Compass, a comprehensive and effective multi-module testing tool for automated testing of DLS under the vast majority of testing requirements. In addition to the essential utility evaluation (including metric evaluation and mutation operations), AI-Compass provides the measurements towards the adversarial robustness, model interpretability, and model's neuron analysis to make an extensive report on the performance of DLS. Furthermore, the feasibility of AI-Compass is tested in multi-modal scenarios. For tasks including image classification, text classification and object detection tasks, AI-Compass shows superior performance and solves the ad-hoc problems of existing testing tools, indicating a high degree of scalability. Extensive experiments demonstrate that AI-Compass is so far the state-of-the-art testing tool to build robust and trustworthy DLS.

Acknowledgement

The work has been supported by the Cyber Security Research Centre Limited whose activities are partially funded by the Australian Government's Cooperative Research Centres Programme.

TABLE 10
The object detection model robustness evaluation results on COCO dataset.

Source Model	Attack Method	Faster R-CNN		RetinaNet		Mask R-CNN		SSD	
		AP	AR	AP	AR	AP	AR	AP	AR
Faster R-CNN	Original	0.585	0.508	0.557	0.537	0.591	0.519	0.415	0.365
	FGSM	0.181	0.179	0.272	0.308	0.258	0.249	0.389	0.345
	I-FGSM	0.051	0.075	0.164	0.239	0.134	0.164	0.394	0.351
	DI-FGSM	0.109	0.146	0.211	0.276	0.189	0.218	0.38	0.34
	TI-FGSM	0.161	0.187	0.321	0.381	0.296	0.31	0.376	0.336
	MI-FGSM	0.041	0.066	0.119	0.178	0.098	0.12	0.375	0.335
	SINI-FGSM	0.038	0.078	0.11	0.196	0.091	0.143	0.35	0.321
	PGD	0.033	0.054	0.114	0.177	0.09	0.114	0.388	0.345
	SAA	0.178	0.197	0.276	0.337	0.263	0.277	0.393	0.351
	Average	0.153	0.166	0.238	0.292	0.223	0.235	0.384	0.343
RetinaNet	Original	0.585	0.508	0.557	0.537	0.591	0.519	0.415	0.365
	FGSM	0.296	0.292	0.169	0.206	0.306	0.305	0.393	0.347
	I-FGSM	0.221	0.264	0.054	0.105	0.233	0.278	0.4	0.355
	DI-FGSM	0.252	0.277	0.111	0.176	0.262	0.289	0.388	0.345
	TI-FGSM	0.372	0.376	0.132	0.212	0.384	0.388	0.386	0.345
	MI-FGSM	0.155	0.198	0.046	0.09	0.166	0.208	0.383	0.34
	SINI-FGSM	0.145	0.2	0.047	0.098	0.157	0.211	0.359	0.326
	PGD	0.166	0.212	0.04	0.08	0.176	0.22	0.395	0.35
	SAA	0.305	0.319	0.162	0.233	0.322	0.335	0.396	0.353
	Average	0.277	0.294	0.146	0.193	0.289	0.306	0.391	0.347

REFERENCES

[1] K. He, X. Zhang, S. Ren, and J. Sun, "Deep residual learning for image recognition," in *Proceedings of the IEEE conference on computer vision and pattern recognition*, 2016, pp. 770–778.

[2] K. Simonyan and A. Zisserman, "Very deep convolutional networks for large-scale image recognition," *arXiv preprint arXiv:1409.1556*, 2014.

[3] W. Xiong, J. Droppo, X. Huang, F. Seide, M. Seltzer, A. Stolcke, D. Yu, and G. Zweig, "Achieving human parity in conversational speech recognition," *arXiv preprint arXiv:1610.05256*, 2016.

[4] J. Chen, K. Hu, Y. Yu, Z. Chen, Q. Xuan, Y. Liu, and V. Filkov, "Software visualization and deep transfer learning for effective software defect prediction," in *Proceedings of the ACM/IEEE 42nd international conference on software engineering*, 2020, pp. 578–589.

[5] P. Devanbu, M. Dwyer, S. Elbaum, M. Lowry, K. Moran, D. Poshyvanyk, B. Ray, R. Singh, and X. Zhang, "Deep learning & software engineering: State of research and future directions," *arXiv preprint arXiv:2009.08525*, 2020.

[6] Y. Li, J. Hua, H. Wang, C. Chen, and Y. Liu, "Deeppayload: Black-box backdoor attack on deep learning models through neural payload injection," in *2021 IEEE/ACM 43rd International Conference on Software Engineering (ICSE)*. IEEE, 2021, pp. 263–274.

[7] A. G. Mirabella, A. Martin-Lopez, S. Segura, L. Valencia-Cabrera, and A. Ruiz-Cortés, "Deep learning-based prediction of test input validity for restful apis," in *2021 IEEE/ACM Third International Workshop on Deep Learning for Testing and Testing for Deep Learning (DeepTest)*. IEEE, 2021, pp. 9–16.

[8] A. Sedaghatbaf, M. H. Moghadam, and M. Saadatmand, "Automated performance testing based on active deep learning," in *2021 IEEE/ACM International Conference on Automation of Software Test (AST)*. IEEE, 2021, pp. 11–19.

[9] B. Xiao and S.-C. Kang, "Development of an image data set of construction machines for deep learning object detection," *Journal of Computing in Civil Engineering*, vol. 35, no. 2, p. 05020005, 2021.

[10] A. Shrestha and A. Mahmood, "Review of deep learning algorithms and architectures," *IEEE access*, vol. 7, pp. 53 040–53 065, 2019.

[11] A. Parvat, J. Chavan, S. Kadam, S. Dev, and V. Pathak, "A survey of deep-learning frameworks," in *2017 International Conference on Inventive Systems and Control (ICISC)*. IEEE, 2017, pp. 1–7.

[12] T. Dhar, N. Dey, S. Borra, and R. S. Sherratt, "Challenges of deep learning in medical image analysis—improving explainability and trust," *IEEE Transactions on Technology and Society*, vol. 4, no. 1, pp. 68–75, 2023.

[13] R. Kavitha, D. K. Jothi, K. Saravanan, M. P. Swain, J. L. A. Gonzáles, R. J. Bhardwaj, E. Adomako *et al.*, "Ant colony optimization-enabled cnn deep learning technique for accurate detection of cervical cancer," *BioMed Research International*, vol. 2023, 2023.

[14] D.-H. Lee and J.-L. Liu, "End-to-end deep learning of lane detection and path prediction for real-time autonomous driving," *Signal, Image and Video Processing*, vol. 17, no. 1, pp. 199–205, 2023.

[15] S. Y. Alaba and J. E. Ball, "Deep learning-based image 3-d object detection for autonomous driving," *IEEE Sensors Journal*, vol. 23, no. 4, pp. 3378–3394, 2023.

[16] D. Haluza and D. Jungwirth, "Artificial intelligence and ten societal megatrends: An exploratory study using gpt-3," *Systems*, vol. 11, no. 3, p. 120, 2023.

[17] P. Maddigan and T. Susnjak, "Chat2vis: Generating data visualisations via natural language using chatgpt, codex and gpt-3 large language models," *IEEE Access*, 2023.

[18] T. Zohdinasab, V. Riccio, A. Gambi, and P. Tonella, "Efficient and effective feature space exploration for testing deep learning systems," *ACM Transactions on Software Engineering and Methodology*, vol. 32, no. 2, pp. 1–38, 2023.

[19] J. Sekhon and C. Fleming, "Towards improved testing for deep learning," in *2019 IEEE/ACM 41st International Conference on Software Engineering: New Ideas and Emerging Results (ICSE-NIER)*. IEEE, 2019, pp. 85–88.

[20] S. Gerasimou, H. F. Eniser, A. Sen, and A. Cakan, "Importance-driven deep learning system testing," in *Proceedings of the ACM/IEEE 42nd International Conference on Software Engineering*, 2020, pp. 702–713.

[21] R. Wadawadagi and V. Pagi, "Sentiment analysis with deep neural networks: comparative study and performance assessment," *Artificial Intelligence Review*, vol. 53, no. 8, pp. 6155–6195, 2020.

[22] Y. Jin, Z. Li, C. Qin, J. Liu, Y. Liu, L. Zhao, and C. Liu, "A novel attentional deep neural network-based assessment method for ecg quality," *Biomedical Signal Processing and Control*, vol. 79, p. 104064, 2023.

[23] M. Alwadi, G. Chetty, and M. Yamin, "A framework for vehicle quality evaluation based on interpretable machine learning," *International Journal of Information Technology*, vol. 15, no. 1, pp. 129–136, 2023.

[24] J. Guo, W. Bao, J. Wang, Y. Ma, X. Gao, G. Xiao, A. Liu, J. Dong, X. Liu, and W. Wu, "A comprehensive evaluation framework for

deep model robustness," *Pattern Recognition*, vol. 137, p. 109308, 2023.

[25] H. K. Gajera, D. R. Nayak, and M. A. Zaveri, "A comprehensive analysis of dermoscopy images for melanoma detection via deep cnn features," *Biomedical Signal Processing and Control*, vol. 79, p. 104186, 2023.

[26] R. Sawhney, A. Malik, S. Sharma, and V. Narayan, "A comparative assessment of artificial intelligence models used for early prediction and evaluation of chronic kidney disease," *Decision Analytics Journal*, vol. 6, p. 100169, 2023.

[27] S. G. Finlayson, H. W. Chung, I. S. Kohane, and A. L. Beam, "Adversarial attacks against medical deep learning systems," *arXiv preprint arXiv:1804.05296*, 2018.

[28] F. Nesti, G. Rossolini, S. Nair, A. Biondi, and G. Buttazzo, "Evaluating the robustness of semantic segmentation for autonomous driving against real-world adversarial patch attacks," in *Proceedings of the IEEE/CVF Winter Conference on Applications of Computer Vision*, 2022, pp. 2280–2289.

[29] T. Gu, B. Dolan-Gavitt, and S. Garg, "Badnets: Identifying vulnerabilities in the machine learning model supply chain," *arXiv preprint arXiv:1708.06733*, 2017.

[30] S. Mehtab and J. Sen, "Analysis and forecasting of financial time series using cnn and lstm-based deep learning models," in *Advances in Distributed Computing and Machine Learning: Proceedings of ICADCML 2021*. Springer, 2022, pp. 405–423.

[31] S. Qiu, M. I. Miller, P. S. Joshi, J. C. Lee, C. Xue, Y. Ni, Y. Wang, I. De Anda-Duran, P. H. Hwang, J. A. Cramer *et al.*, "Multimodal deep learning for alzheimer's disease dementia assessment," *Nature communications*, vol. 13, no. 1, p. 3404, 2022.

[32] Q. Zhang, S. Hu, J. Sun, Q. A. Chen, and Z. M. Mao, "On adversarial robustness of trajectory prediction for autonomous vehicles," in *Proceedings of the IEEE/CVF Conference on Computer Vision and Pattern Recognition*, 2022, pp. 15 159–15 168.

[33] J. Dieber and S. Kirrane, "A novel model usability evaluation framework (muse) for explainable artificial intelligence," *Information Fusion*, vol. 81, pp. 143–153, 2022.

[34] H. Sajjad, N. Durrani, and F. Dalvi, "Neuron-level interpretation of deep nlp models: A survey," *Transactions of the Association for Computational Linguistics*, vol. 10, pp. 1285–1303, 2022.

[35] D. Zhou, Z. Yu, E. Xie, C. Xiao, A. Anandkumar, J. Feng, and J. M. Alvarez, "Understanding the robustness in vision transformers," in *International Conference on Machine Learning*. PMLR, 2022, pp. 27 378–27 394.

[36] E. Dai, T. Zhao, H. Zhu, J. Xu, Z. Guo, H. Liu, J. Tang, and S. Wang, "A comprehensive survey on trustworthy graph neural networks: Privacy, robustness, fairness, and explainability," *arXiv preprint arXiv:2204.08570*, 2022.

[37] Y. Guan, F. Lecue, J. Chen, R. Li, and J. Z. Pan, "Explaining image classification through knowledge-aware neuron interpretation," 2022.

[38] Z. Yang, J. Shi, M. H. Asyrofi, and D. Lo, "Revisiting neuron coverage metrics and quality of deep neural networks," in *2022 IEEE International Conference on Software Analysis, Evolution and Reengineering (SANER)*. IEEE, 2022, pp. 408–419.

[39] N. Pawlowski, S. I. Ktena, M. C. Lee, B. Kainz, D. Rueckert, B. Glocker, and M. Rajchl, "Dltk: State of the art reference implementations for deep learning on medical images," *arXiv preprint arXiv:1711.06853*, 2017.

[40] K. Pei, Y. Cao, J. Yang, and S. Jana, "Deepxplore: Automated whitebox testing of deep learning systems," in *proceedings of the 26th Symposium on Operating Systems Principles*, 2017, pp. 1–18.

[41] Y. Tian, K. Pei, S. Jana, and B. Ray, "Deeptest: Automated testing of deep-neural-network-driven autonomous cars," in *Proceedings of the 40th international conference on software engineering*, 2018, pp. 303–314.

[42] D. Weber, F. Merkle, P. Schöttle, and S. Schlögl, "Less is more: The influence of pruning on the explainability of cnns," *arXiv preprint arXiv:2302.08878*, 2023.

[43] A. Jordao and H. Pedrini, "On the effect of pruning on adversarial robustness," in *Proceedings of the IEEE/CVF International Conference on Computer Vision*, 2021, pp. 1–11.

[44] L. Ma, F. Zhang, J. Sun, M. Xue, B. Li, F. Juefei-Xu, C. Xie, L. Li, Y. Liu, J. Zhao *et al.*, "Deepmutation: Mutation testing of deep learning systems," in *2018 IEEE 29th international symposium on software reliability engineering (ISSRE)*. IEEE, 2018, pp. 100–111.

[45] Q. Hu, L. Ma, X. Xie, B. Yu, Y. Liu, and J. Zhao, "Deepmutation++: A mutation testing framework for deep learning systems," in *2019 34th IEEE/ACM International Conference on Automated Software Engineering (ASE)*. IEEE, 2019, pp. 1158–1161.

[46] Z. Jin, Z. Zhu, H. Hu, M. Xue, and H. Chen, "Poster: Ml-compass: A comprehensive assessment framework for machine learning models," in *Proceedings of the 2023 ACM Asia Conference on Computer and Communications Security*, 2023, pp. 1031–1033.

[47] H. Zheng, Z. Chen, T. Du, X. Zhang, Y. Cheng, S. Ji, J. Wang, Y. Yu, and J. Chen, "Neuronfair: Interpretable white-box fairness testing through biased neuron identification," in *Proceedings of the 44th International Conference on Software Engineering*, 2022, pp. 1519–1531.

[48] L. Ma, F. Juefei-Xu, F. Zhang, J. Sun, M. Xue, B. Li, C. Chen, T. Su, L. Li, Y. Liu *et al.*, "Deepgauge: Multi-granularity testing criteria for deep learning systems," in *Proceedings of the 33rd ACM/IEEE international conference on automated software engineering*, 2018, pp. 120–131.

[49] X. Li, H. Xiong, X. Li, X. Wu, Z. Chen, and D. Dou, "Interpretdl: Explaining deep models in paddlepaddle," *Journal of Machine Learning Research*, vol. 23, no. 197, pp. 1–6, 2022.

[50] M.-I. Nicolae, M. Sinn, M. N. Tran, B. Buesser, A. Rawat, M. Wistuba, V. Zantedeschi, N. Baracaldo, B. Chen, H. Ludwig *et al.*, "Adversarial robustness toolbox v1. 0.0," *arXiv preprint arXiv:1807.01069*, 2018.

[51] I. J. Goodfellow, J. Shlens, and C. Szegedy, "Explaining and harnessing adversarial examples," *arXiv preprint arXiv:1412.6572*, 2014.

[52] S.-M. Moosavi-Dezfooli, A. Fawzi, and P. Frossard, "Deepfool: a simple and accurate method to fool deep neural networks," in *Proceedings of the IEEE conference on computer vision and pattern recognition*, 2016, pp. 2574–2582.

[53] N. Carlini and D. Wagner, "Towards evaluating the robustness of neural networks," in *2017 ieee symposium on security and privacy (sp)*. Ieee, 2017, pp. 39–57.

[54] J. X. Morris, E. Lifland, J. Y. Yoo, J. Grigsby, D. Jin, and Y. Qi, "Textattack: A framework for adversarial attacks, data augmentation, and adversarial training in nlp," *arXiv preprint arXiv:2005.05909*, 2020.

[55] J. Ebrahimi, A. Rao, D. Lowd, and D. Dou, "Hotflip: White-box adversarial examples for text classification," *arXiv preprint arXiv:1712.06751*, 2017.

[56] D. Jin, Z. Jin, J. T. Zhou, and P. Szolovits, "Is bert really robust? a strong baseline for natural language attack on text classification and entailment," in *Proceedings of the AAAI conference on artificial intelligence*, vol. 34, no. 05, 2020, pp. 8018–8025.

[57] J. Rauber, W. Brendel, and M. Bethge, "Foolbox: A python toolbox to benchmark the robustness of machine learning models," *arXiv preprint arXiv:1707.04131*, 2017.

[58] J. Li, S. Ji, T. Du, B. Li, and T. Wang, "Textbugger: Generating adversarial text against real-world applications," *arXiv preprint arXiv:1812.05271*, 2018.

[59] Y. Dong, P. Zhang, J. Wang, S. Liu, J. Sun, J. Hao, X. Wang, L. Wang, J. S. Dong, and D. Ting, "There is limited correlation between coverage and robustness for deep neural networks," *arXiv preprint arXiv:1911.05904*, 2019.

[60] F. Harel-Canada, L. Wang, M. A. Gulzar, Q. Gu, and M. Kim, "Is neuron coverage a meaningful measure for testing deep neural networks?" in *Proceedings of the 28th ACM Joint Meeting on European Software Engineering Conference and Symposium on the Foundations of Software Engineering*, 2020, pp. 851–862.

[61] H. Jin, R. Chen, H. Zheng, J. Chen, Y. Cheng, Y. Yu, T. Chen, and X. Liu, "Excitement surfeited turns to errors: Deep learning testing framework based on excitable neurons," *Information Sciences*, vol. 637, p. 118936, 2023.

[62] X. Li, X. Li, D. Pan, and D. Zhu, "On the learning property of logistic and softmax losses for deep neural networks," in *Proceedings of the AAAI Conference on Artificial Intelligence*, vol. 34, no. 04, 2020, pp. 4739–4746.

[63] M. L. Seltzer, D. Yu, and Y. Wang, "An investigation of deep neural networks for noise robust speech recognition," in *2013 IEEE international conference on acoustics, speech and signal processing*. IEEE, 2013, pp. 7398–7402.

[64] W. Yin, K. Kann, M. Yu, and H. Schütze, "Comparative study of cnn and rnn for natural language processing," *arXiv preprint arXiv:1702.01923*, 2017.

[65] J. Lian, X. Zhou, F. Zhang, Z. Chen, X. Xie, and G. Sun, "xdeepfm: Combining explicit and implicit feature interactions for recommender systems," in *Proceedings of the 24th ACM SIGKDD inter-*

national conference on knowledge discovery & data mining, 2018, pp. 1754–1763.

[66] I. Jindal, M. Nokleby, and X. Chen, "Learning deep networks from noisy labels with dropout regularization," in *2016 IEEE 16th International Conference on Data Mining (ICDM)*. IEEE, 2016, pp. 967–972.

[67] M. Dixon, D. Klabjan, and J. H. Bang, "Classification-based financial markets prediction using deep neural networks," *Algorithmic Finance*, vol. 6, no. 3-4, pp. 67–77, 2017.

[68] S. Guan and M. Loew, "Analysis of generalizability of deep neural networks based on the complexity of decision boundary," in *2020 19th IEEE International Conference on Machine Learning and Applications (ICMLA)*. IEEE, 2020, pp. 101–106.

[69] B. Biggio, I. Corona, D. Maiorca, B. Nelson, N. Šrndić, P. Laskov, G. Giacinto, and F. Roli, "Evasion attacks against machine learning at test time," in *Machine Learning and Knowledge Discovery in Databases: European Conference, ECML PKDD 2013, Prague, Czech Republic, September 23-27, 2013, Proceedings, Part III 13*. Springer, 2013, pp. 387–402.

[70] J. Su, D. V. Vargas, and K. Sakurai, "One pixel attack for fooling deep neural networks," *IEEE Transactions on Evolutionary Computation*, vol. 23, no. 5, pp. 828–841, 2019.

[71] Y. Deng, X. Zheng, T. Zhang, C. Chen, G. Lou, and M. Kim, "An analysis of adversarial attacks and defenses on autonomous driving models," in *2020 IEEE international conference on pervasive computing and communications (PerCom)*. IEEE, 2020, pp. 1–10.

[72] A. Huq and M. T. Pervin, "Analysis of adversarial attacks on skin cancer recognition," in *2020 International Conference on Data Science and Its Applications (ICoDSA)*. IEEE, 2020, pp. 1–4.

[73] A. Kurakin, I. J. Goodfellow, and S. Bengio, "Adversarial examples in the physical world," in *Artificial intelligence safety and security*. Chapman and Hall/CRC, 2018, pp. 99–112.

[74] A. Madry, A. Makelov, L. Schmidt, D. Tsipras, and A. Vladu, "Towards deep learning models resistant to adversarial attacks," *arXiv preprint arXiv:1706.06083*, 2017.

[75] Y. Dong, F. Liao, T. Pang, X. Hu, and J. Zhu, "Discovering adversarial examples with momentum," *arXiv preprint arXiv:1710.06081*, vol. 5, 2017.

[76] Y. Dong, T. Pang, H. Su, and J. Zhu, "Evading defenses to transferable adversarial examples by translation-invariant attacks," in *Proceedings of the IEEE/CVF Conference on Computer Vision and Pattern Recognition*, 2019, pp. 4312–4321.

[77] C. Xiao, B. Li, J.-Y. Zhu, W. He, M. Liu, and D. Song, "Generating adversarial examples with adversarial networks," *arXiv preprint arXiv:1801.02610*, 2018.

[78] H. Li, X. Xu, X. Zhang, S. Yang, and B. Li, "Qeba: Query-efficient boundary-based blackbox attack," in *Proceedings of the IEEE/CVF conference on computer vision and pattern recognition*, 2020, pp. 1221–1230.

[79] P.-Y. Chen, H. Zhang, Y. Sharma, J. Yi, and C.-J. Hsieh, "Zoo: Zeroth order optimization based black-box attacks to deep neural networks without training substitute models," in *Proceedings of the 10th ACM workshop on artificial intelligence and security*, 2017, pp. 15–26.

[80] J. Lin, C. Song, K. He, L. Wang, and J. E. Hopcroft, "Nesterov accelerated gradient and scale invariance for adversarial attacks," *arXiv preprint arXiv:1908.06281*, 2019.

[81] C. Xie, Z. Zhang, Y. Zhou, S. Bai, J. Wang, Z. Ren, and A. L. Yuille, "Improving transferability of adversarial examples with input diversity," in *Proceedings of the IEEE/CVF Conference on Computer Vision and Pattern Recognition*, 2019, pp. 2730–2739.

[82] L. Gao, Q. Zhang, J. Song, X. Liu, and H. T. Shen, "Patch-wise attack for fooling deep neural network," in *Computer Vision–ECCV 2020: 16th European Conference, Glasgow, UK, August 23–28, 2020, Proceedings, Part XXVIII 16*. Springer, 2020, pp. 307–322.

[83] J. Zhang, W. Wu, J.-t. Huang, Y. Huang, W. Wang, Y. Su, and M. R. Lyu, "Improving adversarial transferability via neuron attribution-based attacks," in *Proceedings of the IEEE/CVF Conference on Computer Vision and Pattern Recognition*, 2022, pp. 14 993–15 002.

[84] Y. Long, Q. Zhang, B. Zeng, L. Gao, X. Liu, J. Zhang, and J. Song, "Frequency domain model augmentation for adversarial attack," in *Computer Vision–ECCV 2022: 17th European Conference, Tel Aviv, Israel, October 23–27, 2022, Proceedings, Part IV*. Springer, 2022, pp. 549–566.

[85] Z. Jin, Z. Zhu, X. Wang, J. Zhang, J. Shen, and H. Chen, "Danaa: Towards transferable attacks with double adversarial neuron attribution," *arXiv preprint arXiv:2310.10427*, 2023.

[86] Z. Zhu, H. Chen, J. Zhang, X. Wang, Z. Jin, Q. Lu, J. Shen, and K.-K. R. Choo, "Improving adversarial transferability via frequency-based stationary point search," in *Proceedings of the 32nd ACM International Conference on Information and Knowledge Management*, ser. CIKM '23. New York, NY, USA: Association for Computing Machinery, 2023, p. 3626–3635. [Online]. Available: https://doi.org/10.1145/3583780.3614927

[87] Z. Qin, Y. Fan, Y. Liu, L. Shen, Y. Zhang, J. Wang, and B. Wu, "Boosting the transferability of adversarial attacks with reverse adversarial perturbation," *arXiv preprint arXiv:2210.05968*, 2022.

[88] A. Adadi and M. Berrada, "Peeking inside the black-box: a survey on explainable artificial intelligence (xai)," *IEEE access*, vol. 6, pp. 52 138–52 160, 2018.

[89] M. T. Ribeiro, S. Singh, and C. Guestrin, """ why should i trust you?" explaining the predictions of any classifier," in *Proceedings of the 22nd ACM SIGKDD international conference on knowledge discovery and data mining*, 2016, pp. 1135–1144.

[90] A. Shrikumar, P. Greenside, and A. Kundaje, "Learning important features through propagating activation differences," in *International conference on machine learning*. PMLR, 2017, pp. 3145–3153.

[91] S. M. Lundberg and S.-I. Lee, "A unified approach to interpreting model predictions," *Advances in neural information processing systems*, vol. 30, 2017.

[92] R. C. Fong and A. Vedaldi, "Interpretable explanations of black boxes by meaningful perturbation," in *Proceedings of the IEEE international conference on computer vision*, 2017, pp. 3429–3437.

[93] A. Datta, S. Sen, and Y. Zick, "Algorithmic transparency via quantitative input influence: Theory and experiments with learning systems," in *2016 IEEE symposium on security and privacy (SP)*. IEEE, 2016, pp. 598–617.

[94] J. Li, W. Monroe, and D. Jurafsky, "Understanding neural networks through representation erasure," *arXiv preprint arXiv:1612.08220*, 2016.

[95] R. R. Selvaraju, M. Cogswell, A. Das, R. Vedantam, D. Parikh, and D. Batra, "Grad-cam: Visual explanations from deep networks via gradient-based localization," in *Proceedings of the IEEE international conference on computer vision*, 2017, pp. 618–626.

[96] H. Wang, Z. Wang, M. Du, F. Yang, Z. Zhang, S. Ding, P. Mardziel, and X. Hu, "Score-cam: Score-weighted visual explanations for convolutional neural networks," in *Proceedings of the IEEE/CVF conference on computer vision and pattern recognition workshops*, 2020, pp. 24–25.

[97] A. Patra and J. A. Noble, "Incremental learning of fetal heart anatomies using interpretable saliency maps," in *Annual Conference on Medical Image Understanding and Analysis*. Springer, 2020, pp. 129–141.

[98] J. T. Springenberg, A. Dosovitskiy, T. Brox, and M. Riedmiller, "Striving for simplicity: The all convolutional net," *arXiv preprint arXiv:1412.6806*, 2014.

[99] M. Sundararajan, A. Taly, and Q. Yan, "Axiomatic attribution for deep networks," in *International conference on machine learning*. PMLR, 2017, pp. 3319–3328.

[100] G. Erion, J. D. Janizek, P. Sturmfels, S. M. Lundberg, and S.-I. Lee, "Improving performance of deep learning models with axiomatic attribution priors and expected gradients," *Nature machine intelligence*, vol. 3, no. 7, pp. 620–631, 2021.

[101] Z. Wang, M. Fredrikson, and A. Datta, "Robust models are more interpretable because attributions look normal," *arXiv preprint arXiv:2103.11257*, 2021.

[102] D. Pan, X. Li, and D. Zhu, "Explaining deep neural network models with adversarial gradient integration," in *Thirtieth International Joint Conference on Artificial Intelligence (IJCAI)*, 2021.

[103] Z. Zhu, H. Chen, Z. Jin, X. Wang, J. Zhang, M. Xue, Q. Lu, J. Shen, and K.-K. R. Choo, "Fvw: Finding valuable weight on deep neural network for model pruning," in *Proceedings of the 32nd ACM International Conference on Information and Knowledge Management*, ser. CIKM '23. New York, NY, USA: Association for Computing Machinery, 2023, p. 3657–3666. [Online]. Available: https://doi.org/10.1145/3583780.3614889

[104] S. Ye, K. Xu, S. Liu, H. Cheng, J.-H. Lambrechts, H. Zhang, A. Zhou, K. Ma, Y. Wang, and X. Lin, "Adversarial robustness vs. model compression, or both?" in *Proceedings of the IEEE/CVF International Conference on Computer Vision*, 2019, pp. 111–120.

[105] K. Liu, B. Dolan-Gavitt, and S. Garg, "Fine-pruning: Defending against backdooring attacks on deep neural networks," in *Re-*

search in Attacks, Intrusions, and Defenses: 21st International Symposium, RAID 2018, Heraklion, Crete, Greece, September 10-12, 2018, Proceedings 21. Springer, 2018, pp. 273–294.
[106] Z. Xu, J. Sun, Y. Liu, and G. Sun, "An efficient channel-level pruning for cnns without fine-tuning," in *2021 International Joint Conference on Neural Networks (IJCNN)*. IEEE, 2021, pp. 1–8.
[107] H. Hu, R. Peng, Y.-W. Tai, and C.-K. Tang, "Network trimming: A data-driven neuron pruning approach towards efficient deep architectures," *arXiv preprint arXiv:1607.03250*, 2016.
[108] Y. LeCun, J. Denker, and S. Solla, "Optimal brain damage," *Advances in neural information processing systems*, vol. 2, 1989.
[109] P. Molchanov, A. Mallya, S. Tyree, I. Frosio, and J. Kautz, "Importance estimation for neural network pruning," in *Proceedings of the IEEE/CVF conference on computer vision and pattern recognition*, 2019, pp. 11 264–11 272.
[110] H. Wang, C. Qin, Y. Zhang, and Y. Fu, "Neural pruning via growing regularization," *arXiv preprint arXiv:2012.09243*, 2020.
[111] G. Retsinas, A. Elafrou, G. Goumas, and P. Maragos, "Weight pruning via adaptive sparsity loss," *arXiv preprint arXiv:2006.02768*, 2020.
[112] A. Kapishnikov, S. Venugopalan, B. Avci, B. Wedin, M. Terry, and T. Bolukbasi, "Guided integrated gradients: An adaptive path method for removing noise," in *Proceedings of the IEEE/CVF conference on computer vision and pattern recognition*, 2021, pp. 5050–5058.
[113] V. Petsiuk, A. Das, and K. Saenko, "Rise: Randomized input sampling for explanation of black-box models," *arXiv preprint arXiv:1806.07421*, 2018.
[114] A. Krizhevsky, G. Hinton *et al.*, "Learning multiple layers of features from tiny images," 2009.
[115] T.-Y. Lin, M. Maire, S. Belongie, J. Hays, P. Perona, D. Ramanan, P. Dollár, and C. L. Zitnick, "Microsoft coco: Common objects in context," in *Computer Vision–ECCV 2014: 13th European Conference, Zurich, Switzerland, September 6-12, 2014, Proceedings, Part V 13*. Springer, 2014, pp. 740–755.
[116] R. Socher, A. Perelygin, J. Wu, J. Chuang, C. D. Manning, A. Y. Ng, and C. Potts, "Recursive deep models for semantic compositionality over a sentiment treebank," in *Proceedings of the 2013 conference on empirical methods in natural language processing*, 2013, pp. 1631–1642.
[117] Y. Kim, "Convolutional neural networks for sentence classification," *arXiv preprint arXiv:1408.5882*, 2014.
[118] Z. Liu, W. Zhou, and H. Li, "Ab-lstm: Attention-based bidirectional lstm model for scene text detection," *ACM Transactions on Multimedia Computing, Communications, and Applications (TOMM)*, vol. 15, no. 4, pp. 1–23, 2019.
[119] S. Ren, K. He, R. Girshick, and J. Sun, "Faster r-cnn: Towards real-time object detection with region proposal networks," *Advances in neural information processing systems*, vol. 28, 2015.
[120] T.-Y. Lin, P. Goyal, R. Girshick, K. He, and P. Dollár, "Focal loss for dense object detection," in *Proceedings of the IEEE international conference on computer vision*, 2017, pp. 2980–2988.
[121] W. Li, X. Wang, H. Han, and J. Qiao, "A pls-based pruning algorithm for simplified long–short term memory neural network in time series prediction," *Knowledge-Based Systems*, vol. 254, p. 109608, 2022.

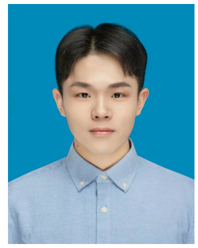

Zhiyu Zhu is currently pursuing the Master degree at the University of Sydney, he is also an Honours Student at CSIRO Data61. His research interests encompass AI model security and Trustworthy Machine Learning.

Zhibo Jin received his bachelor's degree from China University of Petroleum (Beijing) and is currently pursuing a Master's degree at the University of Sydney. He is also an Honours Student at CSIRO Data61. His research focuses on AI model security and Trustworthy Machine Learning.

Hongsheng Hu Hongsheng Hu received his PhD degree at Faculty of Engineering, University of Auckland, New Zealand. His research focuses on AI privacy and security, especially membership inference attacks, differential privacy, and inference attacks in the context of federated learning. He has published 8 international refereed journal and conference papers, including ACM Computing Surveys, IJCAI, and ICDM.

Minhui Xue received the Ph.D. degree from East China Normal University, Shanghai, China. He is currently a Senior Research Scientist with CSIRO's Data61, Marsfield, NSW, Australia. He is also an Honorary Lecturer with Macquarie University, Sydney, NSW, Australia. His current research interests include machine learning security and privacy, system security and privacy, and Internet measurement. Dr. Xue was a recipient of the ACM Special Interest Group on Software Engineering (ACM CCS) Best Paper Award Runner-Up and the ACM Special Interest Group on Software Engineering (SIGSOFT) Distinguished Paper Award. He serves or has served on the Program Committees of the 2021 and 2023 IEEE Symposium on Security and Privacy; the 2022 and 2023 ACM Conference on Computer and Communications Security; the 2023 and 2024 USENIX Security Symposium (USENIX) Security Symposium; the 2023 and 2024 Network and Distributed System Security Symposium; and the 2021, 2022, and 2023 ACM/IEEE International Conference on Software Engineering.

Ruoxi Sun received the Ph.D. degree with The University of Adelaide, Adelaide, SA, Australia. He is a Research Fellow with CSIRO's Data61, Marsfield, NSW, Australia. His work in the cybersecurity and privacy domains has led to the publication of over ten papers in leading conferences and journals, such as the IEEE Symposium on Security and Privacy (S&P), ACM Conference on Computer and Communications Security (CCS), Network and Distributed System Security Symposium (NDSS), The Web Conference (WWW), International Conference on Software Engineering (ICSE), The ACM Joint European Software Engineering Conference and Symposium on the Foundations of Software Engineering (ESEC/FSE), The IEEE/ACM Automated Software Engineering Conference (ASE), Annual Conference on Neural Information Processing Systems (NeurIPS), and others. His research interests include mobile security and privacy, the Internet of Things (IoT) security, and machine learning security.

Seyit Camtepe Dr Seyit Camtepe received his PhD in Computer Science from Rensselaer Polytechnic Institute (America's oldest technological research university), New York, USA 2007. From 2007 to 2013, he was a Senior Researcher and Team Leader focusing on AI and Cyber Security at the TU-Berlin (the first German university to adopt the name ”Technische Universität”), Germany. He worked as an ECARD lecturer at the QUT, Australia, for five years. As part of these roles, he led or participated in many large impactful projects (i.e., multi-national and with more than five partners/countries) in Europe funded by the European Commission and in Australia, supported by industry and government. He completed CSIRO's Experienced Leader Program (ELP) and Spark Leader Labs to mature his leadership skills on top of the leadership skills he built over 27 years on three continents. He has been a PC member in prestigious ML and Cyber security conferences such as ESORICS, ASIACCS, AAAI and ECML-PKDD. He was a co-editor of a special issue on Cryptography: A Cyber Security Toolkit.

Praveen Gauravaram Praveen has a PhD in Cryptology from Queensland University of Technology, Brisbane, Australia and has held scientific positions in India, Europe, and Australia and is a recipient of research grants and awards whist his research fellowship at Technical University of Denmark. Praveen was a recipient of young elite scientist award in 2010 from the Danish Agency for Science, Technology, and Innovation for his contributions to research in Cryptographic Hash Functions. Praveen has more than sixty publications and consulting advisories in cyber security. Praveen is professionally passioned about engaging customers in emerging technologies for customer business growth and successful digital transformation. Praveen holds honorary academic titles of Adjunct Associate Professor with the School of Computer Science and Engineering, Faculty of Engineering at UNSW and Adjunct Professor with the School of Information Technology, Faculty of Science, Engineering and Built Environment at Deakin University. Praveen is also an Advisor for the ICT Curriculum Advisory Group of Southern Cross University. Praveen enjoys playing weekend cricket, daily morning walks, and Aussie outdoors.

Huaming Chen (Member, IEEE) received the Ph.D. degree from the University of Wollongong, Wollongong, Australia. He is currently a senior lecturer with the School of Electrical and Computer Engineering, the University of Sydney, Sydney, Australia. His main research interests include software engineering/security, trustworthy AI, and applied machine learning. He is the organiser of TRUSTWORTHY AND RESPONSIBLE AI workshop. He serves on the program committees of ACM MM, CCS, IJCAI, KDD, The Web Conference, SIAM ICDM, ECML/PKDD and so on.